



HAL
open science

Solvent effect investigation on the acid-catalyzed esterification of levulinic acid by ethanol aided by a Linear Solvation Energy Relationship

Sindi Baco, Marcel Klinksiek, Rashid Ismail Bedawi Zakaria, Elizabeth Antonia Garcia-Hernandez, Mélanie Mignot, Julien Legros, Christoph Held, Valeria Casson Moreno, Sébastien Leveneur

► To cite this version:

Sindi Baco, Marcel Klinksiek, Rashid Ismail Bedawi Zakaria, Elizabeth Antonia Garcia-Hernandez, Mélanie Mignot, et al.. Solvent effect investigation on the acid-catalyzed esterification of levulinic acid by ethanol aided by a Linear Solvation Energy Relationship. Chemical Engineering Science, In press, pp.117928. 10.1016/j.ces.2022.117928 . hal-03735962

HAL Id: hal-03735962

<https://normandie-univ.hal.science/hal-03735962>

Submitted on 21 Jul 2022

HAL is a multi-disciplinary open access archive for the deposit and dissemination of scientific research documents, whether they are published or not. The documents may come from teaching and research institutions in France or abroad, or from public or private research centers.

L'archive ouverte pluridisciplinaire **HAL**, est destinée au dépôt et à la diffusion de documents scientifiques de niveau recherche, publiés ou non, émanant des établissements d'enseignement et de recherche français ou étrangers, des laboratoires publics ou privés.

Solvent effect investigation on the acid-catalyzed esterification of levulinic acid by ethanol aided by a Linear Solvation Energy Relationship

Sindi Baco^{1,3,¥}, Marcel Klinksiak^{2,¥}, Rashid Ismail Bedawi Zakaria^{1,4}, Elizabeth Antonia Garcia-Hernandez¹, Mélanie Mignot³, Julien Legros³, Christoph Held², Valeria Casson Moreno⁴, Sébastien Leveneur^{1*}

¹*INSA Rouen, UNIROUEN, Normandie Univ, LSPC, UR4704, 76000 Rouen, France, E-mail*: sebastien.leveneur@insa-rouen.fr*

²*Laboratory of Thermodynamics, Department of Biochemical and Chemical Engineering, TU Dortmund University, Emil-Figge. Str.70, 44227 Dortmund, Germany*

³*INSA Rouen, CNRS, Normandie Université, UNIROUEN, COBRA laboratory, F-76000 Rouen, France*

⁴*Dipartimento di Ingegneria Chimica, Civile, Ambientale e dei Materiali, Alma Mater Studiorum—Università di Bologna, via Terracini 28, 40131 Bologna, Italy*

[¥] These authors contributed equally to the work.

Abstract

When processing lignocellulosic biomass materials to obtain platform molecules such as levulinic acid (LA), alkyl levulinates or γ -valerolactone (GVL), the choice of solvent is of prime importance for kinetics. The knowledge of relationships between reaction kinetics and solvent serves as a decision tool for process design. To determine such relationships, esterification reactions was chosen because such reaction steps are present in several biomass conversion processes. In this work, kinetic models of LA esterification by ethanol over sulfuric acid in polar aprotic solvent (GVL) and polar protic solvents (water or ethanol) were developed and evaluated by Bayesian statistics. The apparent dissociation constants in solvents were estimated by ePC-SAFT approach to distinguish the proton concentration from the rate constants. The developed models can fit the experimental concentrations of ethyl levulinate and predict the proton concentration. Using the Kamlet-Abboud-Taft equation, linear relationships between estimated rate constants and solvent properties were established at different temperatures. We observed that solvents with low polarizability and high bond acceptor capacity should be favored for this reaction. Hence, the reaction of esterification is faster in ethanol solvent than in GVL solvent than in water solvent.

Keywords

Esterification, Kinetic modeling, Bayesian statistics, ethyl levulinate, ePC-SAFT, Kamlet-Abboud-Taft equation.

1. Introduction

The development of lignocellulosic biomass (LCB) valorization processes is growing because this substrate is renewable, abundant, and not competing with the alimentary sector. The shift from fossil-based refineries to biorefineries is challenging due to the diversity of biomass structures (Singhvi and Gokhale, 2019), the biomass gathering and seasonability (Pyrgakis and Kokossis, 2018), the pretreatment complexity for LCB fractionation (Zhao et al., 2022), the identification of platform molecules (Shinde et al., 2019), the need to discover new catalysts (Singhvi and Gokhale, 2019), etc.

Alkyl levulinate (AL) and levulinic acid (LA) are promising platform molecules issued from cellulose and hemicellulose hydrolysis or alcoholysis. The hydrogenation of AL or LA leads to the production of γ -valerolactone (GVL), which is also a platform molecule (Alonso et al., 2013; Capecchi et al., 2021a, 2021b; Piskun et al., 2016; Wang et al., 2019; Yan et al., 2015). In the fuel sector, alkyl levulinates are used as fuel oxygenate additives or as blending components for diesel (Peixoto et al., 2021; Peng et al., 2015), improving the fuel quality and reducing pollutant emission (Joshi et al., 2011; Windom et al., 2011). In 2017, Tian et al. showed that methyl and ethyl levulinates have higher anti-knock quality than Euro95 gasoline (Tian et al., 2017).

Production of alkyl levulinate is commonly done through the esterification of LA (Badgajar et al., 2020). The other production route is via the alcoholysis of monosaccharide or biomass-derived furanic compounds reducing the side production of humins compared to water solvolysis (Bhat et al., 2021; Di Menno Di Bucchianico et al., 2022; Li et al., 2016; van Zandvoort et al., 2013).

From a chemistry and chemical engineering viewpoint, we need to address the transformation challenges of LCB into valuable chemicals. The tryptic kinetics-catalyst-thermodynamics is fundamental to find the optimal operating conditions, i.e., using less energy, being safe, and providing the maximum of target chemicals quickly.

In this perspective, the role of solvent or reaction mixture is fundamental if we want to succeed in the biomass-industry shift. A solvent can interfere with the kinetics and thermodynamics of a reaction system. In 2014, Mellmer et al. (Mellmer et al., 2014) showed that aprotic polar solvent could improve the catalytic activity of protons. They suggested that the polar aprotic solvent can change the stabilization of the acidic proton relative to the protonated transition state during the acid-catalyzed conversion of xylose into furfural. They proposed to express the rate constant by using the Gibbs energy for proton solvation. Nevertheless, such thermodynamic data can be cumbersome to estimate. In 1981, Kamlet et al. (Kamlet et al., 1981) developed a linear relationship between the solvent effect and the reaction kinetics. This equation, also known as Kamlet-Abboud-Taft equation (KAT), considers three solvent properties: its dielectric behavior, solvent ability to donate protons and electrons. This approach requires the knowledge of solvatochromic parameters (Islam et al., 2020; Jessop et al., 2012; Laurence et al., 2015; Lu et al., 2002a; Nikolć et al., 2010; Sherwood et al., 2019).

KAT was used to evaluate the solvent effect on spectral properties of compounds (Aaron et al., 1996, 1995; Párkányi et al., 1993; Rauf et al., 2012), on molecule solubility or solvent-solute interactions (Holzweber et al., 2013; Marcus, 2006; Paul et al., 2013; Thadathil et al., 2019; Wu et al., 2007), on radical scavenging activity (Jabbari and Gharib, 2012) or on reaction kinetics (Auxenfans et al., 2017; García-Río et al., 1997; Raducan et

al., 2012; Ušcumlić and Nikolić, 2009). Nevertheless, the use of this approach in kinetics at different reaction temperatures is seldom. The study of Lu et al. (Lu et al., 2002b) on the hydrolysis of nitroaromatic compounds in different solvents and temperatures can be cited.

Catalyst studies for ALs synthesis via esterification or transesterification are vast (Da Silva et al., 2021; Melchiorre et al., 2020; Russo et al., 2020; Zainol et al., 2019). While the number of research papers on the solvent effect in esterification is relatively significant (Janssen et al., 1999; Lemberg and Sadowski, 2017; Liu et al., 2006; Lotti et al., 2015; Riechert et al., 2015), there are just a few of them concerning the solvent effect for the esterification of LA (Di et al., 2019). The study of Di et al. (Di et al., 2019) was on the esterification of methyl levulinate over immobilized enzyme, and they showed that enzymatic activity is lower when the hydrogen-bond forces of the solvent are strong. Thus, hydrophobic solvents (i.e., ionic liquids) are preferred. However, they did not quantify the contribution of polarizability, hydrogen donor and acceptor on the kinetics.

The present work aims at developing three kinetic models for the synthesis of ethyl levulinate (EL) from LA in GVL solvent (polar aprotic), ethanol solvent (polar protic) and in water solvent (polar protic). These kinetic models, assessed by Bayesian inference, allowed a fair comparison between solvents. KAT approach cannot predict the acid dissociation constant in different solvents. Thus, the acid dissociation constants were estimated by ePC-SAFT equation of state (Voges et al., 2016). The knowledge of acid dissociation constants allows quantifying the proton concentration contribution to the rate constant. Esterification kinetic and thermodynamic constants in the three solvents were

estimated via non-linear regression (Delgado et al., 2022; Stewart and Caracotsios, 2008).

The last stage was using kinetic constants in different solvents and at different temperatures in KAT equations to understand the solvent effect on kinetics.

2. Material and methods

2.1 Chemicals

The following chemicals were used without further purification: γ -valerolactone (wt% \geq 99%) and LA (wt% \geq 97%), both purchased from Sigma Aldrich. Ethanol absolute (wt% \geq 99,7%) and acetone (wt% \geq 99,8 vol%) were supplied by VWR Chemicals. Finally, ethyl levulinate (wt% \geq 98%) was purchased from Acros Organics and sulfuric acid (wt% \geq 98%) was obtained from Honeywell Fukla Chemicals. Distilled water was used.

2.2 Analytical method

GC-FID was used to measure the concentration of EL. The apparatus is BrukerScion GC436 equipped with a flame ionization detector, an autosampler, and a capillary column (ZB5, 30 m x 0.32 mm x 0.25 μ m). Helium (99.99%) was the carrier gas used at a constant flow rate of 1.2 mL min⁻¹ to transfer the sample from the injector, through the column, and into the FID-detector. The temperature of the injector and the detector were set at 250°C, while the program temperature of the oven was as follows: from 50°C (1 min) to 200°C (1 min) at 20°C min⁻¹. The injection volume was 1 μ L and the split ratio was 1:20.

During the reaction, different samples were collected and diluted with acetone up to a dilution factor of 10000. In this way, a very low concentration of H₂SO₄ was present in the GC column, avoiding any damage. To evaluate the EL concentration in samples, calibration curves were done between 0 mg L⁻¹ to 100 mg L⁻¹ of EL.

2.3 Experimental procedure

Esterification reaction was carried out in a 300 mL glass reactor vessel, operating in batch mode. It was equipped with a jacket, in which water circulated and heated using a thermostat. A condenser was present to avoid mass loss due to the evaporation, and water was the cooling fluid. The pressure inside the reactor was equal to the atmospheric pressure. The presence of a mechanical stirrer was required in order to obtain a homogeneous reaction mixture. The stirrer was fixed at 450 rpm. Samples at different time intervals were taken by a plastic syringe through a reactor neck during a reaction.

For the performed kinetic experiments, starting solutions with only one reactant were poured into the reactor, and the temperature was brought to the desired reaction temperature prior to the addition of the preheated second reactant. The starting solutions were an aqueous solution of LA (or EL) and H_2SO_4 in water solvent, non-aqueous GVL solution of LA (or EL) and H_2SO_4 in GVL solvent reactions, and non-aqueous H_2SO_4 in ethanol solvent. The preheated second reactant added was ethanol in water solvent and GVL solvent reactions, while LA was in ethanol solvent. A typical reaction mass was ca. 230 grams, and the total sampling weight percentage was lower than 15%.

Tables 1, 2 and 3 show the experimental matrix for the kinetic experiments performed in the GVL, ethanol and water solvents. Besides probing solvent influences on the reaction, the operating conditions were varied for reaction temperature, catalyst, reactant, and product initial concentrations to develop robust kinetic models. For experiments in ethanol solvent, the maximum reaction temperature was fixed to 70°C because of the ethanol boiling point, which is ca. 78°C at 1 bar.

Table 1. Experimental matrix for kinetic experiments in GVL solvent.

Run	Temp	[H ₂ SO ₄] ₀	[EL] ₀	[LA] ₀	[Ethanol] ₀	[GVL] ₀	[Water] ₀
	°C	mol.L ⁻¹	mol.L ⁻¹	mol.L ⁻¹	mol.L ⁻¹	mol.L ⁻¹	mol.L ⁻¹
1	80.0	0.04	0.00	2.27	9.01	1.89	0.00
2	70.0	0.05	0.00	2.30	9.11	1.94	0.00
3	60.0	0.09	0.00	2.30	9.12	2.03	0.00
4	50.0	0.09	0.00	2.33	9.19	2.02	0.00
5	70.0	0.04	0.00	3.39	6.88	2.13	0.00
6	80.0	0.04	0.00	3.34	6.74	2.12	0.00
7	60.0	0.04	0.00	2.33	9.21	1.93	0.00
8	60.0	0.09	0.00	2.32	9.19	1.90	0.00
9	60.0	0.09	0.00	2.30	9.21	1.83	0.54
10	60.0	0.09	0.00	2.34	9.18	1.63	1.60
11	60.0	0.09	0.07	3.32	9.20	0.85	0.00
12	60.0	0.09	0.40	2.32	9.20	1.34	0.00
13	60.0	0.09	0.00	2.32	9.19	1.94	0.00
14	60.0	0.09	0.00	2.32	9.17	1.19	4.05
15	80.0	0.07	0.00	2.72	8.18	1.91	0.00
16	50.0	0.07	0.00	2.84	8.48	1.93	0.00

Table 2. Experimental matrix for kinetic experiments in water solvent.

Run	Temp °C	[H ₂ SO ₄] ₀ mol.L ⁻¹	[EL] ₀ mol.L ⁻¹	[LA] ₀ mol.L ⁻¹	[Ethanol] ₀ mol.L ⁻¹	[Water] ₀ mol.L ⁻¹
1W	60.0	0.09	0.00	2.33	9.21	10.28
2W	60.0	0.04	0.00	2.33	9.23	10.30
3W	50.0	0.09	0.00	2.33	9.23	10.72
4W	80.0	0.04	0.00	2.33	9.23	9.22
5W	70.0	0.04	0.00	3.33	6.83	11.58
6W	50.0	0.07	0.00	2.69	8.06	11.05
7W	80.0	0.04	0.00	3.37	6.72	11.79
8W	80.0	0.07	0.00	2.23	8.88	10.92
9W	70.0	0.00	0.00	3.41	6.82	11.84
10W	60.0	0.09	0.07	2.25	8.99	10.85
11W	60.0	0.09	0.00	2.28	9.09	10.93
12W	70.0	0.09	0.00	3.39	6.78	11.80
13W	50.0	0.04	0.00	2.31	9.23	10.93
14W	80.0	0.09	0.00	2.67	8.02	11.23
15W	50.0	0.09	0.00	2.76	8.29	11.35

Table 3. Experimental matrix for kinetic experiments in ethanol solvent.

Run	Temp °C	[H ₂ SO ₄] ₀ mol.L ⁻¹	[EL] ₀ mol.L ⁻¹	[LA] ₀ mol.L ⁻¹	[Ethanol] ₀ mol.L ⁻¹	[Water] ₀ mol.L ⁻¹
1E	50.0	0.09	0.00	2.88	11.51	0.00
2E	60.0	0.09	0.00	2.85	11.38	0.00
3E	70.0	0.09	0.00	2.82	11.25	0.00
4E	60.0	0.04	0.00	2.86	11.41	0.00
5E	60.0	0.07	0.00	2.76	11.40	0.00
6E	50.0	0.07	0.00	2.88	11.53	0.00
7E	50.0	0.07	0.00	3.39	10.48	0.00
8E	50.0	0.07	0.00	4.45	8.83	0.00
9E	60.0	0.090	0.00	2.85	11.38	0.00

2.4 Prediction of apparent dissociation constants with ePC-SAFT advanced

The electrolyte Perturbed-Chain Statistical Associating Fluid Theory (ePC-SAFT) developed by Cameretti and Sadowski (Cameretti et al., 2005) is an extension of the original PC-SAFT equation of state from Gross and Sadowski (Gross and Sadowski, 2001) to model electrolyte solutions. ePC-SAFT includes electrostatic long-range interactions among ions expressed by Debye-Hückel theory.

ePC-SAFT was used to estimate the dissociation constants of sulfuric acid in GVL and ethanol solvents by calculating the activity coefficients γ_i . A detailed description of this approach can be found in Supplementary Materials (S1). Dissociation constants (pK_a) of acids in mixtures of aqueous and organic solvents are indistinct. The modeling aims to determine reliable values of the dissociation constant of H_2SO_4 in water, ethanol and GVL with the use of ePC-SAFT advanced. For the theoretical evaluation, the equilibrium constant $K_{th,1}$ of the first and second dissociation $K_{th,2}$ need to be calculated.



Reaction equilibria for any chemical reaction, also for dissociation reactions, are characterized by the activity-based equilibrium constant K_{th} . The equilibrium constant is calculated with the mole fractions and activity coefficients of the reactants and products according to Eq. (3).

$$K_{th}(T, p) = K_x(T, p, x) \cdot K_\gamma(T, p, x) = \prod_i (x_i \cdot \gamma_i)^{\nu_i} \quad (3)$$

K_{th} depends neither on the type nor on the concentration of the solvent. The dependence on reaction conditions is taken into account by the activity coefficients γ_i . Thus, once the equilibrium constant is known, it can be used to predict the equilibrium concentrations in any other solvent or solvent mixture. K_x is also known as the mole-fraction ratio at equilibrium, or sometimes also denoted apparent equilibrium constant; any concentration scale can be used instead of mole fractions. In the literature, the concentration-based value K_c is typically used to determine the apparent dissociation constant pK_a^c by Eq. (5). The latter is not exactly the same as the standard value for pK_a^a , which is true only assuming that activity coefficients of products and reactants cancel out.

$$pK_a^a = -\log_{10} K_{th} \quad (4)$$

$$pK_a^c = -\log_{10} K_c \quad (5)$$

However, activity coefficients might crucially depend on the kind of solvent. The related value K_γ requires knowledge about rational activity coefficients γ_i^* . For all species, the infinite dilution in pure water was applied as a reference state to calculate the activity coefficients γ_i^* . The equilibrium constant $K_{th,1}$ and $K_{th,2}$ for each dissociation step is defined according to Eq. (3) as follows:

$$K_{th,1} = \frac{x_{H^+} \cdot x_{HSO_4^-}}{x_{H_2SO_4}} \cdot \frac{\gamma_{H^+}^* \cdot \gamma_{HSO_4^-}^*}{\gamma_{H_2SO_4}^*} \rightarrow K_{x,1} = \frac{x_{H^+} \cdot x_{HSO_4^-}}{x_{H_2SO_4}} = K_{th,1} \cdot \left(\frac{\gamma_{H^+}^* \cdot \gamma_{HSO_4^-}^*}{\gamma_{H_2SO_4}^*} \right)^{-1} \quad (6)$$

$$K_{th,2} = \frac{x_{H^+} \cdot x_{SO_4^{2-}}}{x_{HSO_4^-}} \cdot \frac{\gamma_{H^+}^* \cdot \gamma_{SO_4^{2-}}^*}{\gamma_{HSO_4^-}^*} \rightarrow K_{x,2} = \frac{x_{H^+} \cdot x_{SO_4^{2-}}}{x_{HSO_4^-}} = K_{th,2} \cdot \left(\frac{\gamma_{H^+}^* \cdot \gamma_{SO_4^{2-}}^*}{\gamma_{HSO_4^-}^*} \right)^{-1} \quad (7)$$

The pK_a^x values are then the negative logarithm (to the base of 10) of the K_x value, which allows easy conversion to K_c and pK_a^c , respectively. Thus, the activity coefficients of the ions are required. These were modeled in this work with the thermodynamic equation of state ePC-SAFT advanced (Bülow et al., 2021) (S1).

2.5 Kinetic modeling

Athena Visual Studio (Stewart and Caracotsios, 2008) was used to solve the ordinary differential equations-algebraic equations and estimate kinetic, equilibrium and Kamlet-Abboud-Taft parameters. This software uses Bayesian inference to analyze the estimated parameters. The GREGLUS package, implemented in Athena, can provide optimal parameter estimates with the 95% confidence intervals, expressed by the highest probability density (HPD). GREGPLUS provides the normalized parameter covariance matrix. Ordinary differential equations ODEs and algebraic equations were solved simultaneously by the solver DDALPUS algorithm, via a damped Newton method, implemented in Athena (Caracotsios and Stewart, 1985).

2.6 Kamlet-Abboud-Taft (KAT) equation

There is a distinction between non-specific and specific solute-solvent interactions in the KAT approach. The latter interaction, i.e., the solute-solvent specific interactions, comprises solvent Lewis-acidity and solvent Lewis-basicity interactions. The relationship between the rate constant in a solvent $k_C^{Solvent}$ and the solvent properties is expressed in Eq. 8 (Kamlet et al., 1981; Nikolć et al., 2010; Weiß et al., 2021).

$$\ln(k_C^{Solvent}) = A_0 + s \cdot \pi^* + a \cdot \alpha + b \cdot \beta \quad (8)$$

where, the terms π^* , α and β are solvatochromic solvent parameters that were supposed to be temperature independent in this study. The solvatochromic parameter α measures the solvent hydrogen-bond donor (HBD) acidity and evaluates the ability of a solvent to release a proton in a solvent to solute hydrogen bond. The values of α vary from zero (e.g., non-HBD solvents) to 1.0 (e.g., methanol). The solvatochromic parameter π^* is an index of solvent dipolarity/polarizability, representing the ability of the solvent to stabilize a charge or a dipole via its dielectric effect. The values of π^* vary from 0.00 for cyclohexane to 1.00 for dimethylsulfoxide. The solvatochromic parameter β measures the solvent hydrogen-bond acceptor (HBA) basicity, and evaluates the solvent ability to accept a proton in a solute-to-solvent hydrogen bond. The β -scale values are from zero for non-HBD solvents to 1 for hexamethylphosphoric acid triamide (HMPT).

The term A_0 is the regression value. The regression coefficients (a, b, and s) present the relative susceptibilities of the solvent dependence of $\ln(k_C^{Solvent})$ to the solvent parameters. Table 4 displays the solvatochromic solvent parameters for each solvent/environmental condition used in this study (Islam et al., 2020). Athena visual studio was used to estimate a, b and s via DDAPLUS solver (Stewart and Caracotsios, 2008).

Table 4. Solvatochromic solvent parameters (Islam et al., 2020).

	π^* [-]	α [-]	β [-]
GVL	0.9	0	0.6
Water	1.2	1.2	0.5
Ethanol	0.6	0.9	0.8

3 Results and discussion

For the sake of clarity, several phenomenological results were put in Supplementary Materials.

3.1 Phenomenological analysis

Classical experiments to evaluate repeatability (Figs S2.1 & S2.2 & S2.3), temperature effect (Figs S2.4 & S2.5 & S2.6) and catalyst effect (Figs S2.7 & S2.8 & S2.9) were performed for water solvent, GVL solvent and ethanol solvent. It was observed that the used procedure is repeatable, that the increase of temperature and catalyst leads to accelerate the reaction rate. In the absence of sulfuric acid, the kinetics was observed to be very slow and negligible in any solvents at 70°C. For these reasons, such experiments were discarded in the modeling stage.

A priori, water could affect sulfuric acid dissociation when GVL is used as a solvent. Fig. 1 shows that the increase of water concentration decreases the kinetics of EL synthesis, meaning that water is not needed to catalyze this reaction over sulfuric acid. Based on this experimental observation, proton in GVL solvent was expressed in (H^+) state and not in the hydroxonium ion (H_3O^+). In ethanol solvent, proton was also expressed in (H^+) state. This observation was also done by Liu et al. (Liu et al., 2006), who observed an inhibition effect of water on sulfuric acid for the esterification of acetic acid by methanol.

In Fig. 1 and the other, the error bar represents the standard deviation, and each sample was analyzed three times.

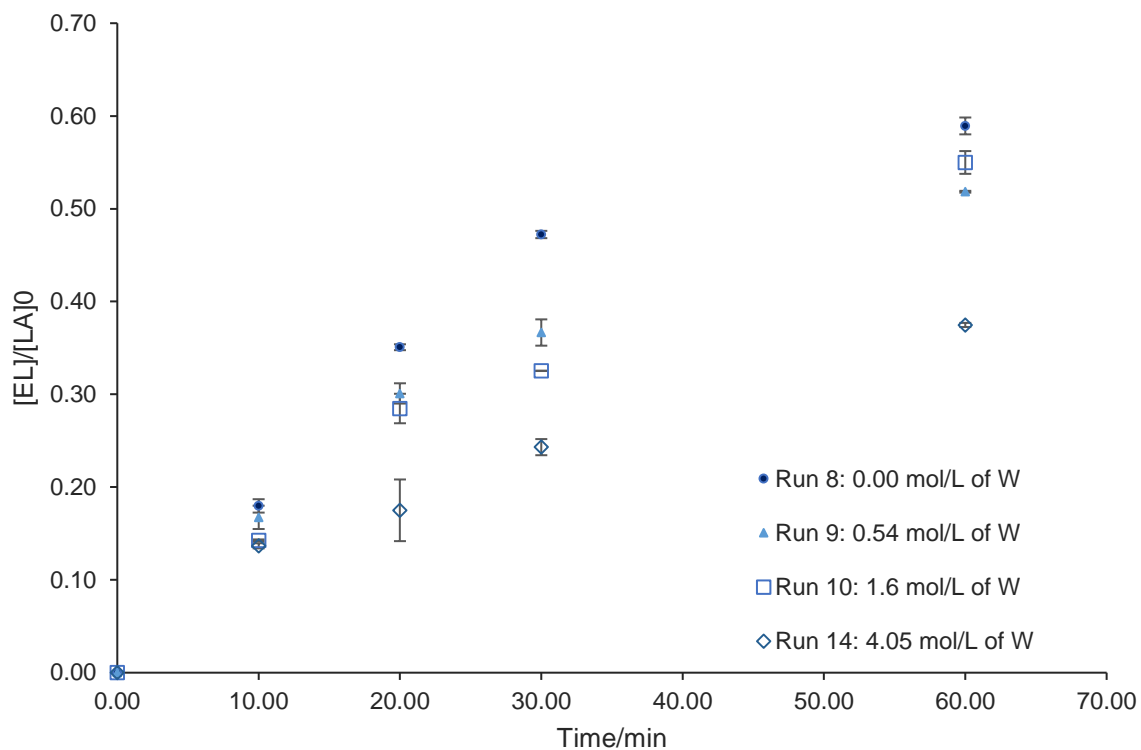


Fig. 1. Effect of water concentration on the kinetics of esterification by comparing Runs 8, 9, 10 and 14 at 60 °C and $[H_2SO_4]_0$: 0.09 mol.L⁻¹.

3.2 Solvent effect on the dissociation constant pK_a^c

The key to predict the dissociation constant in non-aqueous solutions is the equilibrium constant K_{th} . The availability of the thermodynamically consistent equilibrium constant K_{th} allows predicting solvent effects on K_c values and thus on the dissociation equilibrium. The acidity of an acid is expressed as dissociation constant pK_a^c . Because of the complications of measuring the acidity in non-aqueous solvents or mixtures with organic solvents and because of the fact that such data is missing for acids in many organic solvents, it is necessary to reliably predict the experimentally accessible pK_a^c values. In order to apply this procedure to H_2SO_4 , the pK_a^c values of H_2SO_4 in water, $pK_a^c(solvent = water, T = 298.15 K, p = 1 bar) = -3$ (Kolthoff and Elving, 1959; Williams, 2022), was used as an input value to calculate K_{th} at the same temperature and pressure using the ePC-SAFT advanced predicted activity coefficients referred to an infinite dilution state in pure water according to Eq.(S1.8). This K_{th} value was then kept constant (at the considered temperature and pressure), but new activity coefficients for the species of H_2SO_4 in the organic solvent were required to obtain pK_a^c in organic solvents. These were predicted by means of ePC-SAFT advanced using Eq. (S1.8), i.e., relating the ion's fugacity coefficient at infinite dilution in organic solvent to the infinite-dilution reference state in pure water. Based on this, a K_γ value was obtained, which finally yielded K_c and pK_a^c using the afore-determined constant K_{th} (Eq. (3)). The same procedure was done for both dissociation steps. The calculated $K_{th,2}$ for the second dissociation by ePC-SAFT using $pK_{a,2}^c = 1.96$ (Izutsu, 2009) results to 0.0174, and is in proper agreement with the literature value of 0.0119 published by Sippola and Sippola and Taskinen (Sippola, 2013; Sippola and Taskinen, 2014). Further, the calculated dissociation constants for the second step $pK_{a,2}^c$ in

different solvents are in good agreement with literature data (DMSO $pK_{a,2,ePC-SAFT}^c = 16.3$, $pK_{a,2,Lit.}^c = 14.7$ (Izutsu, 2009)) and DMF $pK_{a,2,ePC-SAFT}^c = 18.3$, $pK_{a,2,Lit.}^c = 17.2$ (Izutsu, 2009)). The dissociation of the second step is very low therefore, the focus is on the first dissociation step in organic media via ePC-SAFT approach. The resulting pK_a^c values in five different solvents at 298.15 K and 1 bar are shown in Fig. 2.

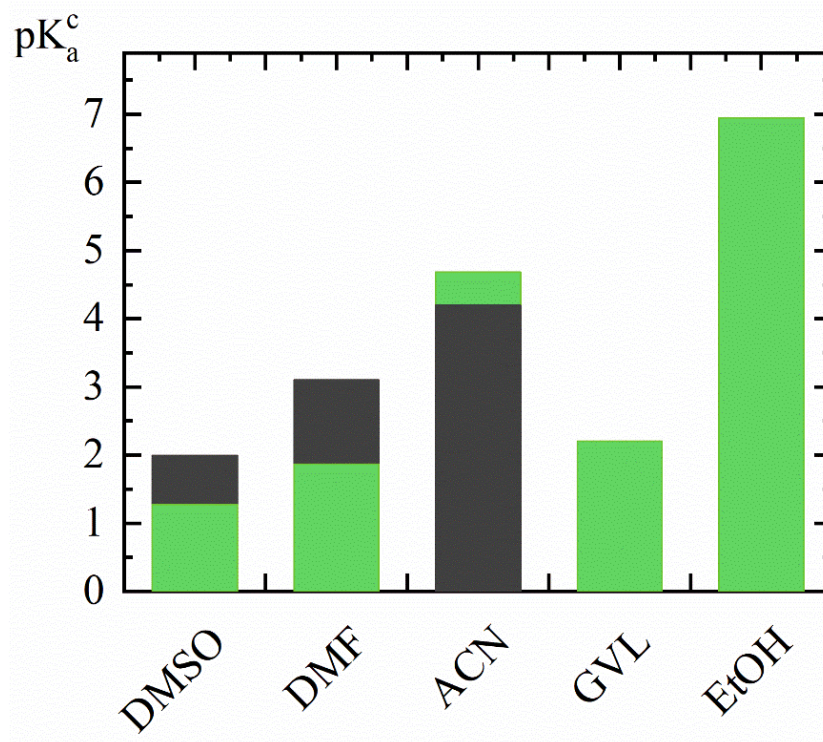


Fig. 2. pK_a^c values of H_2SO_4 in various solvents at 298.15 K and 1 bar. Literature values in dark grey (Izutsu, 2009; Kolthof and Chantooni, 1999), ePC-SAFT predictions using the parameters from Tables S1 - S3 in light green.

Fig. 2 compares the literature pK_a^c values of H_2SO_4 in DMSO, DMF and ACN at 298.15 K and 1 bar (Izutsu, 2009; Kolthof and Chantooni, 1999) with ePC-SAFT advanced modeling. It can be seen that ePC-SAFT advanced is well validated by the experimental data. The modeling results shown in Fig. 2 are obtained without any adjustment of the binary interaction parameters k_{ij} . With literature pK_a^c values, it is possible to fit the binary interaction parameter between protons and organic solvents. For DMSO and DMF the prediction is in agreement with the literature with $k_{ij} = 0.17$ and $k_{ij} = 0.177$, respectively. The dissociation of H_2SO_4 is mainly determined by the differences of the dielectric constants of organic solvent to water. This procedure allowed reliable modeling results of pK_a^c values of H_2SO_4 in DMSO, DMF and ACN (Fig. 2). Thus, the same strategy was applied to predict pK_a^c values of H_2SO_4 in GVL and ethanol. The first dissociation constant of sulfuric acid based on concentration in GVL results to $9.13 \cdot 10^{-3} \text{ mol.L}^{-1}$, whereas the

one in ethanol is even lower with $1.12 \cdot 10^{-7} \text{ mol.L}^{-1}$ (Table S.1.4). This clarifies, that the dissociation is significantly reduced in organic solvents.

Additionally, Fig. 2 reveals the influence of the dielectric constant ($\epsilon_{r,DMSO} = 46.45$, $\epsilon_{r,DMF} = 36.7$, cf. Table S3.1) on the dissociation constants in DMSO ($pK_a^c = 1.99$) and DMF ($pK_a^c = 3.1$).

In the following, we described our approach to determine the dissociation constant value for the second dissociation of sulfuric acid in water and in GVL solvent, the dissociation constant of LA in GVL and in water. In this study, the first dissociation of sulfuric acid in water was considered to be total, the second dissociation constant of sulfuric acid and the one of LA in ethanol was neglected based on the ePC-SAFT analysis.

Shen et al. have observed that DMF (*N,N*-dimethylformamide) and GVL have similar dielectric constant values (Shen et al., 2019). Hence, dissociation constants in DMF solvent are similar than those in GVL solvent (Izutsu, 2003).

Table S1.4 shows the values of dissociation constants for sulfuric acid, its second dissociation, acetic acid, benzoic acid and LA in different solvents (Izutsu, 2003). The first dissociation constant of sulfuric acid in DMF is lower than in water. The second sulfuric acid dissociation constant is higher in water solvent, whereas it is very low in DMF solvent. The dissociation constant of LA in water was found from the work of Kopetzki et al. (Kopetzki and Antonietti, 2010) and Piskun et al. (Piskun et al., 2016). To the best of our knowledge, there are no data concerning the dissociation of LA in non-aqueous solvents like GVL, DMF. In this study, the effect of temperature on the dissociation constant was supposed to be negligible.

The following notations are introduced: K_I , K_{II} and K_{III} , represent the apparent constants of the first dissociation of sulfuric acid, the second dissociation of sulfuric acid, and the dissociation of LA, respectively

In GVL solvent, the following values for the dissociation constants were used: K_I : $9.13 \cdot 10^{-03} \text{ mol.L}^{-1}$ from ePC-SAFT approach; K_{II} : $6.31 \cdot 10^{-18} \text{ mol.L}^{-1}$ as the one found in DMF solvent (Table S1.4) and K_{III} : $3.00 \cdot 10^{-13} \text{ mol.L}^{-1}$. The latter value K_{III} , the dissociation constant of LA in GVL solvent, was evaluated as an average one between the dissociation constant of acetic and benzoic acids in DMF. In ethanol solvent, K_I was estimated to be $1.12 \cdot 10^{-07} \text{ mol.L}^{-1}$ from ePC-SAFT approach, and K_{II} and K_{III} were found to be negligible.

Knopf et al. have developed an expression for the dissociation reaction of the bisulfate ion (Knopf et al., 2003) ($HSO_4^- \leftrightarrow SO_4^{2-} + H^+$) in aqueous H_2SO_4 solutions. In the experimental conditions of Knopf et al., the sulfuric acid concentration is low; therefore, the activity coefficient of the solutions is close to unity. By dividing the apparent second dissociation from (Knopf et al., 2003) by the water concentration in the case of high dilution, i.e., 55.5 mol.L^{-1} , the apparent second dissociation constant for sulfuric acid can be obtained.

In water solvent, the following values for the dissociation constants were used: $K_{II} = \frac{0.011}{55.5}$ and $K_{III} = \frac{2.57 \cdot 10^{-5}}{55.5}$. The value of K_{II} was calculated as an average value between 50 and 80°C , and the value K_{III} was obtained from Piskun et al. (Piskun et al., 2016).

In sum, Table 5 displays the values of K_I , K_{II} and K_{III} used in this study in the different solvents.

Table 5. Values of K_I , K_{II} and K_{III} used in this study.

	GVL solvent	EtOH solvent	Water solvent
K_I (first dissociation of H_2SO_4)	$9.13 \cdot 10^{-03} \text{ mol.L}^{-1}$	$1.12 \cdot 10^{-07} \text{ mol.L}^{-1}$	Infinity
K_{II} (second dissociation of H_2SO_4)	$6.31 \cdot 10^{-18} \text{ mol.L}^{-1}$	0 mol.L^{-1}	$\frac{0.011}{55.5}$
K_{III} (dissociation of LA)	$3.00 \cdot 10^{-13} \text{ mol.L}^{-1}$	0 mol.L^{-1}	$\frac{2.57 \cdot 10^{-5}}{55.5}$

3.3 Kinetic modeling

3.3.1 Mechanism

Figs S4.1 and S4.2 illustrate reaction mechanisms in GVL, water and ethanol solvents. The esterification reaction of LA by ethanol in the presence of an acid catalyst, as H_2SO_4 , can be divided into three main steps:

- Proton production (Steps 1 to 5 from Figs S4.1 and S4.2),
- Catalyzed route due to the activation of the carbonyl groups by protons (Steps 6-8 from Figs S4.1 and S4.2),
- Non-catalyzed route (Steps 9-12 from Figs S4.1 and S4.2).

Our group used this approach to model the hydrolysis of acetic anhydride (Garcia-Hernandez et al., 2019). A quasi-equilibrium hypothesis was used to determine the concentration of protons from sulfuric acid and LA dissociation and determine the concentrations of some intermediates.

3.3.2 Kinetic expressions

In Supplementary Material, the reader can find the derivation of the kinetic expressions in GVL, ethanol, and water solvents (S5).

In GVL solvent and ethanol solvent

For the catalyzed route, the quasi-equilibrium assumption was applied to the reversible proton donor steps 6 and 8 (Fig. S4.1). The rate-determining step is reversible step 7 (Fig. S4.1). The rate of esterification in GVL solvent can be derived as

$$r_{esterification}^{GVL} = k_c^{GVL} \cdot [H^+] \cdot \left([LA] \cdot [EtOH] - \frac{1}{K_c^{GVL}} \cdot [EL] \cdot [H_2O] \right) \quad (9)$$

The rate of esterification in ethanol solvent can be expressed as

$$r_{esterification}^{Ethanol} = k_c^{Ethanol} \cdot [H^+] \cdot \left([LA] \cdot [EtOH] - \frac{1}{K_c^{Ethanol}} \cdot [EL] \cdot [H_2O] \right) \quad (10)$$

In the modeling stage, $k_c^{GVL}(T_{ref})$, E_a^{GVL} , $k_c^{Ethanol}(T_{ref})$ and $E_a^{Ethanol}$ were estimated.

In water solvent

For the catalyzed route, the quasi-equilibrium assumption was applied to the reversible proton donor steps 6 and 8 (Fig. S4.2). The rate-determining step is reversible step 7 (Fig. S4.2), and the rate of esterification can be expressed as

$$r_{esterification}^W = k_c^W \cdot \frac{[H_3O^+]}{[H_2O]} \cdot \left([LA] \cdot [EtOH] - \frac{1}{K_c^W} \cdot [EL] \cdot [H_2O] \right) \quad (11)$$

In the modeling stage, we estimated $k_c^W(T_{ref})$ and E_a^W .

3.3.3 Expression of the apparent equilibrium constant

In the low sulfuric acid concentration range used in this study, the apparent equilibrium constant (calculated based on concentrations) was supposed not to be affected by the sulfuric acid concentration itself. Hence, apparent equilibrium constants calculated based on the concentration can be assumed to be the true thermodynamic equilibrium constants. The effect of temperature on the true thermodynamic equilibrium constant is described by the law of Van't Hoff equation:

$$\frac{d\ln(K(T))}{dT} = \frac{\Delta H_r^0}{RT^2} \quad (12)$$

where, ΔH_r^0 stands for the standard reaction enthalpy change. Assuming that ΔH_r^0 is independent from T, the integration of Eq.(12) from a reference temperature T_{ref} to an arbitrary temperature T leads to:

$$\ln \frac{K(T)}{K(T_{ref})} = \frac{-\Delta H_r^0}{R} \left(\frac{1}{T} - \frac{1}{T_{ref}} \right) \quad (13)$$

In the modelling stage, $K_c^{Solvent}(T_{ref})$ and $\Delta H_r^{Solvent}$ were estimated for each solvent.

3.3.4 Calculation of protons concentration

In order to facilitate reading, the derivation of concentration expression for the three solvents was described in detail in Supplementary Materials (S6). Autoprotolysis of water and ethanol was neglected in the three solvents. To determine the proton concentration, molar balances on sulfate and organic species were performed, and the electroneutrality principle was used.

Calculation of proton concentrations in GVL solvent and ethanol solvent

In these solvents, the expression for the proton concentration is:

$$[H^+] = \frac{K_I \frac{[H_2SO_4]_0}{[H^+]} + 2 \cdot K_I \cdot K_{II} \cdot [H_2SO_4]_0 \cdot \left(\frac{1}{[H^+]}\right)^2}{1 + K_I \frac{1}{[H^+]} + K_I \cdot K_{II} \frac{1}{[H^+]^2}} + \frac{K_{III} \frac{1}{[H^+]} \cdot ([LA]_0 - [EL])}{1 + K_{III} \frac{1}{[H^+]}} \quad (14)$$

The initial proton concentration was calculated by neglecting K_{II} and K_{III} .

Calculation of proton concentrations in water solvent

The first dissociation of sulfuric acid (K_I) in water solvent tends to infinity. Thus, the implicit expression for the hydroxonium concentration is:

$$\frac{[H_2O]}{[H_3O^+]} \frac{[H_2SO_4]_0}{\frac{[H_2O]}{[H_3O^+]} + K_{II} \frac{[H_2O]^2}{[H_3O^+]^2}} + 2 * K_{II} \frac{[H_2O]^2}{[H_3O^+]^2} \frac{[H_2SO_4]_0}{\frac{[H_2O]}{[H_3O^+]} + K_{II} \frac{[H_2O]^2}{[H^+]^2}} + K_{III} \frac{[H_2O]}{[H_3O^+]} * \frac{[LA]_0 - [EL]}{1 + K_{III} \frac{[H_2O]}{[H_3O^+]}} = [H_3O^+] \quad (15)$$

The initial hydroxonium concentration was calculated using the same approach as in the reference (Leveneur et al., 2008). This leads to:

$$[H_3O^+] = \frac{1}{2} \cdot [H_2SO_4]_0 + \sqrt{\frac{[H_2SO_4]_0^2}{4} + 2 \cdot K_{II} \cdot [H_2SO_4]_0 \cdot [H_2O] + K_{III} \cdot [H_2O] \cdot [LA]} \quad (16)$$

The solver DDAPLUS algorithm was used during the modeling stage to determine the proton concentration by solving Eqs (14) and (15).

3.3.5 Material balances and modeling results

The rate equation is expressed by Eqs (9), (10) or (11). Material balances in solvents are:

$$\frac{dC_{LA}}{dt} = -r_{esterification} \quad (17)$$

$$\frac{dC_{Ethanol}}{dt} = -r_{esterification} \quad (18)$$

$$\frac{dC_{EL}}{dt} = r_{esterification} \quad (19)$$

$$\frac{dC_W}{dt} = r_{esterification} \quad (20)$$

Ordinary differential equations ODEs (17)-(20) and algebraic equations (14) or (15) were solved simultaneously by the solver DDALPUS algorithm (Caracotsios and Stewart, 1985). During the parameter estimation stage, the GREGPLUS package minimizes the objective function $S(\theta)$, and can calculate the maximum posterior probability density of the different estimated parameters θ and the values of the posterior distribution of the tested models.

$$S(\theta) = \sum_{u=1}^n ([y_u - f_u(\theta)])^2 \quad (21)$$

where, y_u and $f_u(\theta)$ are experimental and simulated concentrations of EL, respectively.

A modified Arrhenius equation was used to express the rate constants during the modeling stage to ease the parameter identification and decrease the correlation between the pre-exponential factor and activation energy (Buzzi-Ferraris, 1999).

$$k_c(T) = \exp \left[\ln \left(k_c(T_{ref}) \right) + \frac{E_a}{R \cdot T_{ref}} \cdot \left(1 - \frac{T_{ref}}{T} \right) \right] \quad (22)$$

where, T_{ref} is a reference temperature which is the average temperature of the experimental matrix.

The apparent equilibrium constant was linearized as

$$K_c(T) = \exp \left[\ln \left(K_c(T_{ref}) \right) + \frac{\Delta H_r}{R \cdot T_{ref}} \cdot \left(1 - \frac{T_{ref}}{T} \right) \right] \quad (23)$$

The following constants were estimated: $\ln \left(k_c(T_{ref}) \right)$, $\frac{E_a}{R \cdot T_{ref}}$, $\ln \left(K_c(T_{ref}) \right)$ and $\frac{\Delta H_r}{R \cdot T_{ref}}$.

Kinetic modeling results in GVL solvent

Table 6 shows the values of the estimated apparent constants with a reference temperature of 64 °C for the kinetic constant. One can notice that the credible intervals for each estimated constant are short, meaning that the experimental matrix was well designed (Table 1). Esterification of LA by ethanol in GVL solvent is an endothermic system. The values of $k_c^{GVL}(T_{ref})$, E_a^{GVL} , $K_c^{GVL}(T_{ref})$ and ΔH_r^{GVL} are displayed in Table S7.1. Table S7.2 shows that correlations between the estimated constants are very low, meaning that the estimated constants were well identified.

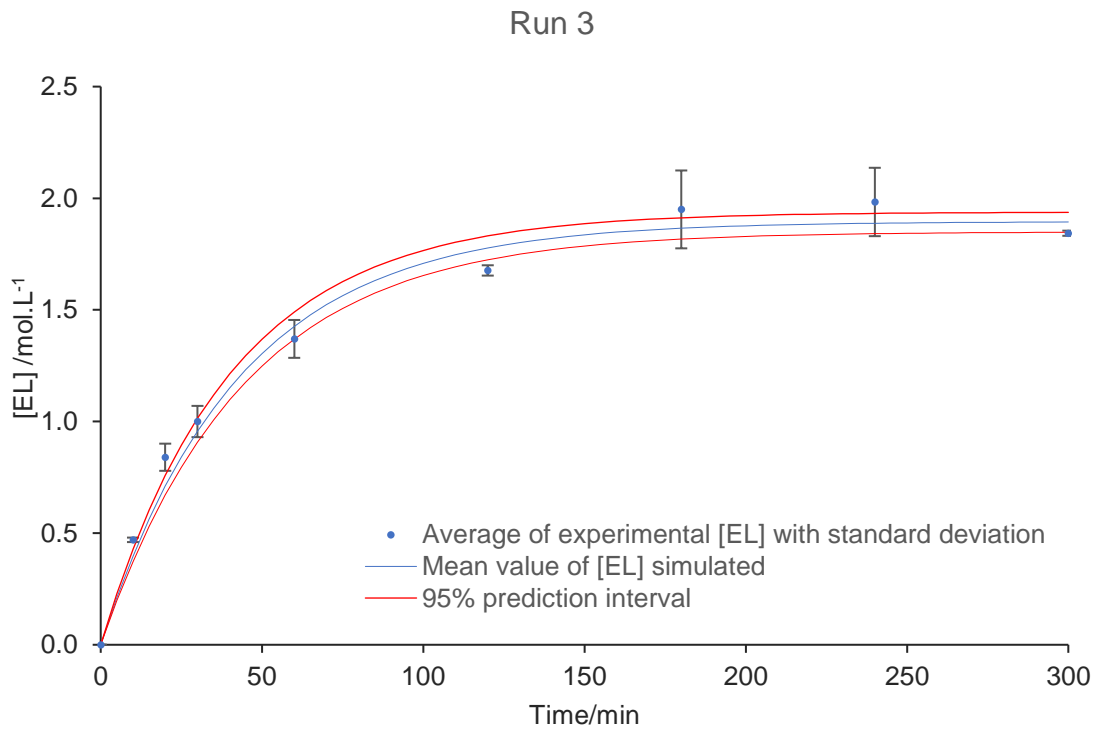
Table 6. Estimated values at $T_{ref}=64$ °C and statistical data for esterification in GVL solvent.

	Units	Estimated value	95% marginal HPD intervals	HDP in %
$\ln(k_c^{GVL}(T_{ref}))$	$L^2 \cdot mol^{-2} \cdot min^{-1}$	-2.22	0.05	2.40
$\frac{E_a^{GVL}}{R \cdot T_{ref}}$	-	18.06	1.84	10.21
$\ln(K_c^{GVL}(T_{ref}))$	-	0.39	0.11	28.17
$\frac{\Delta H_r^{GVL}}{R \cdot T_{ref}}$	-	15.49	4.34	28.00

Globally, the parity plot (Fig. S7.1) shows that the developed model fits well the experimental concentration of EL.

The residual analysis (Figs S7.2-S7.5) shows that the residuals are normally distributed versus the events, time, simulated and experimental EL concentrations. These normal distributions confirm that the developed model is correct.

Fig. 3 shows the fit of the model to some experimental concentrations of EL with the 95% prediction intervals and the mean estimated values. From Fig. 3, one can notice that the model fits well the experimental concentrations, and most of the experimental concentrations lie between the intervals. The developed model can correctly predict the initial kinetics and the equilibrium phase.



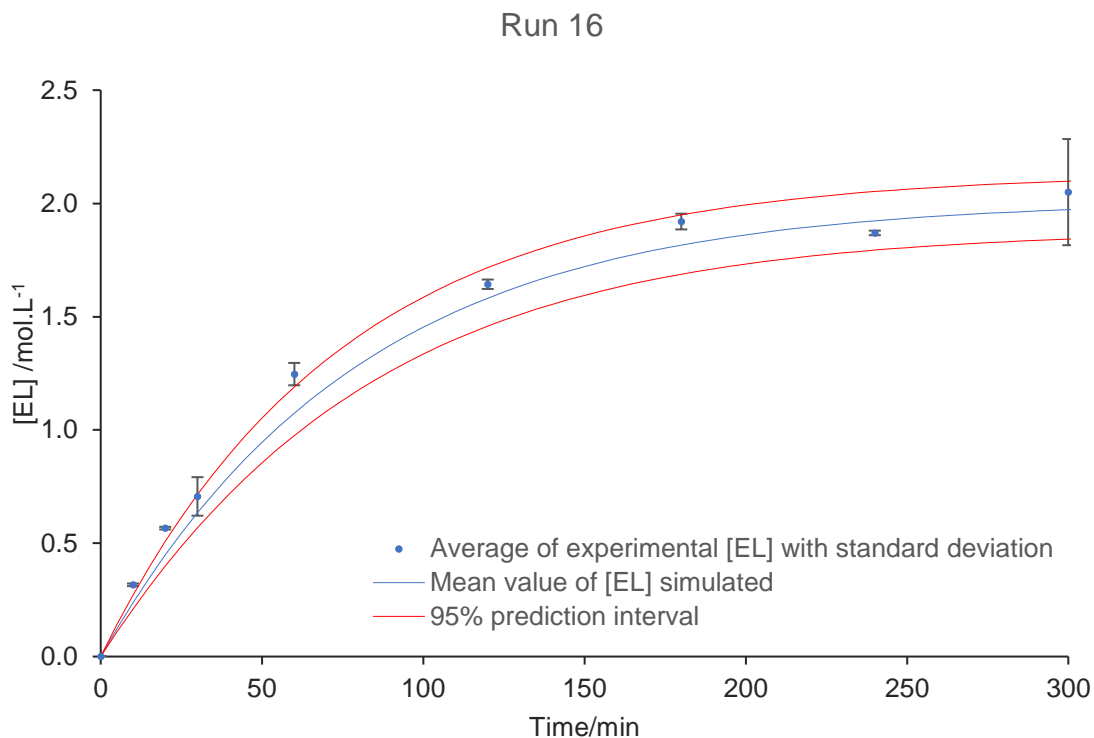


Fig. 3. Fit of Model to the experimental concentrations with prediction intervals for the synthesis of EL in GVL solvent.

Kinetic modeling results in ethanol solvent

Table 7 shows the values of the estimated constants with a reference temperature of 57 °C. As in the previous case, it can be noticed that the credible interval for each estimated constant is short (except for $\Delta H_r^{Ethanol}$) showing the good design of the experimental matrix (Table 3). The values of $k_c^{Ethanol}(T_{ref})$, $E_a^{Ethanol}$, $K_c^{Ethanol}(T_{ref})$ and $\Delta H_r^{Ethanol}$ are displayed in Table S7.3. Table S7.4 shows the correlations between the estimated constants. In general, the correlation between estimated parameters is very low, except for, $K_c^{Ethanol}(T_{ref})$ and $\Delta H_r^{Ethanol}$, which is 0.857. Nevertheless, according to Toch et al. (Toch et al., 2015), two parameters are correlated if the binary correlation coefficient is

higher than 0.95. Thus, the estimated parameters can be considered non-correlated in this case.

Table 7. Estimated values at $T_{ref}=57$ °C and statistical data for esterification in ethanol solvent.

	Units	Estimated value	95% marginal HPD intervals	HDP in %
$\ln(K_c^{Ethanol}(T_{ref}))$	$L^2 \cdot mol^{-2} \cdot min^{-1}$	2.91	0.06	1.95
$\frac{E_a^{Ethanol}}{R \cdot T_{ref}}$	-	24.26	2.84	11.72
$\ln(K_c^{Ethanol}(T_{ref}))$	-	1.49	0.43	28.81
$\frac{\Delta H_r^{Ethanol}}{R \cdot T_{ref}}$	-	42.32	23.14	54.68

Fig. S7.6 shows the parity plot of the ethanol solvent. With an $R^2 = 0.94$, it is possible to ascertain that the model fits well the experimental data for EL.

The residual analysis (Figs S7.7-S7.10) shows that the residuals are normally distributed versus the events, time, simulated and experimental EL concentrations. These normal distributions confirm that the developed model is well-expressed.

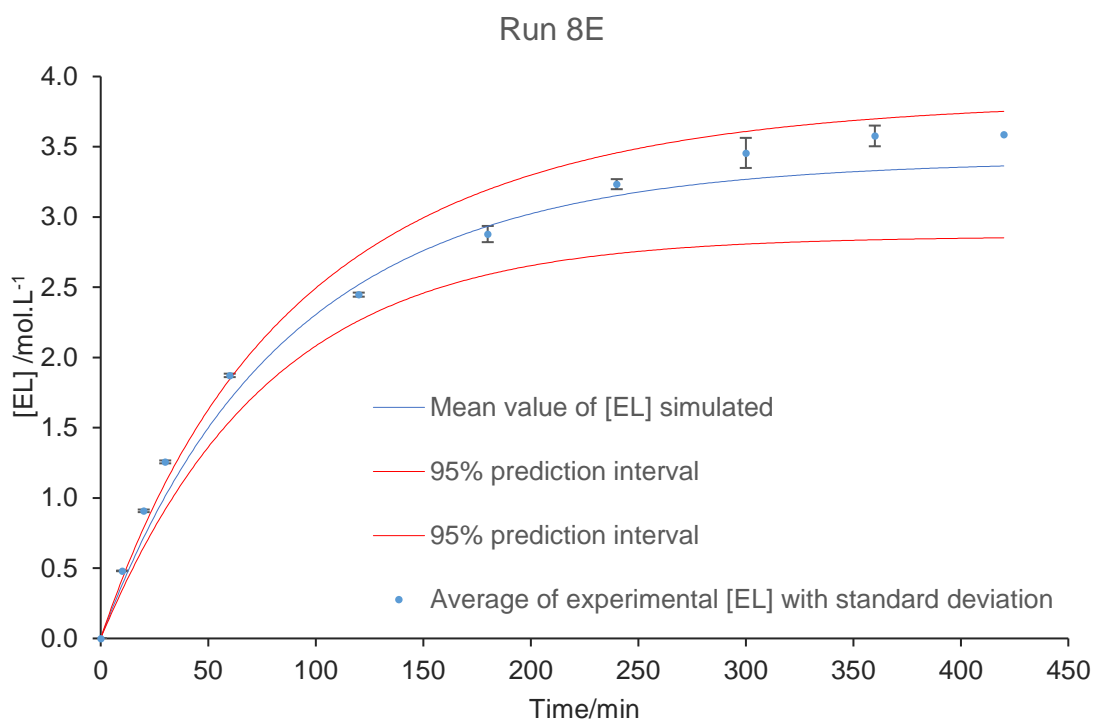
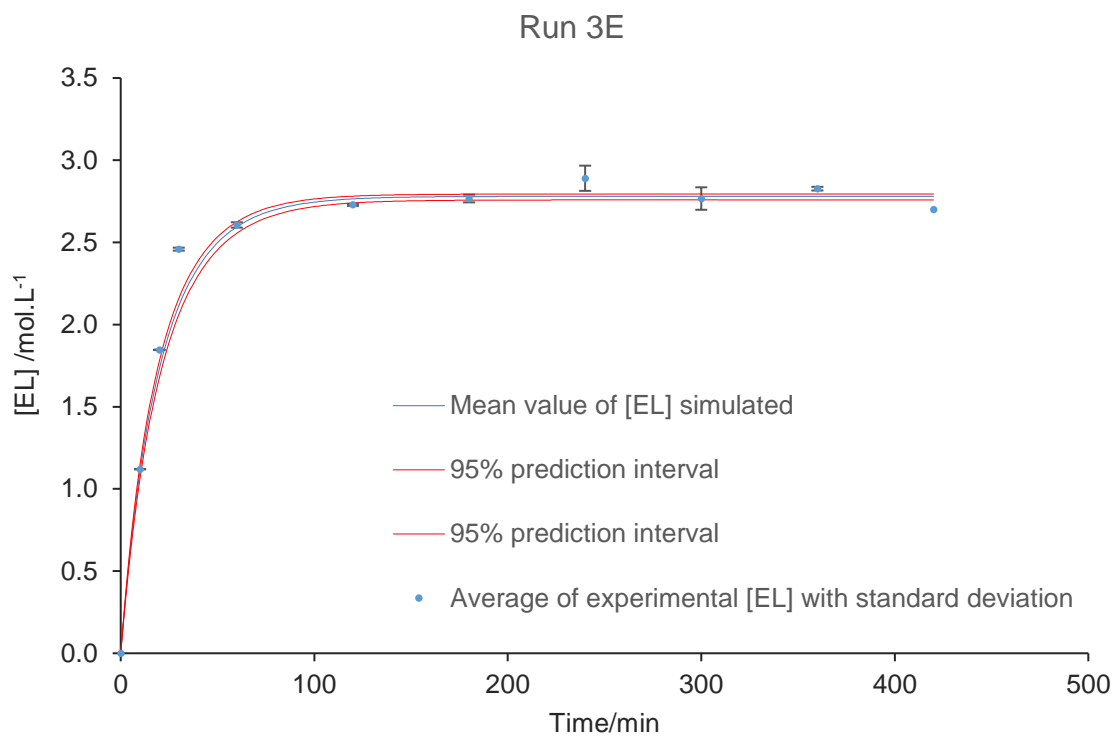


Fig. 4. Fit of model to the experimental concentrations with prediction intervals for the solvent-free synthesis of EL in ethanol solvent.

Fig. 4 shows the fit of the model to some experimental concentrations of EL with the 95% prediction intervals and the mean estimated values. As in the system with GVL solvent, it is possible to confirm that the model fits well the experimental concentrations, and most of the experimental concentrations lie between the intervals. The initial kinetics and the equilibrium phase are well predicted with this model.

Kinetic modeling results in water solvent

Table 8 shows the values of the estimated constants with a reference temperature of 64 °C for the kinetic constants. One can notice that the credible intervals for each estimated constant are narrow. The values of $k_c^W(T_{ref})$, E_a^W , $K_c^W(T_{ref})$ and ΔH_r^W are displayed in Table S7.5. Esterification of LA by ethanol in water solvent is an endothermic system.

Table S7.6 shows that correlations between the estimated constants are low in general. Nevertheless, the correlations between $\ln(k_c^W(T_{ref}))$ and $\ln(K_c^W(T_{ref}))$; $\frac{\Delta H_r^W}{R \cdot T_{ref}}$ and $\frac{E_a^W}{R \cdot T_{ref}}$ can be qualified as medium, but lower than 0.95. Hence, the medium correlation observed for these estimated parameters did not result in wrong identification.

Table 8. Estimated values at $T_{ref}=64$ °C and statistical data for esterification in water solvent.

	Units	Estimated value	95% marginal HPD intervals	HDP in %
$\ln(k_c^W(T_{ref}))$	L.mol ⁻¹ .min ⁻¹	-2.46	0.08	3.27
$\frac{E_a^W}{R \cdot T_{ref}}$	-	21.82	2.42	11.10
$\ln(K_c^W(T_{ref}))$	-	1.14	0.18	15.71
$\frac{\Delta H_r^W}{R \cdot T_{ref}}$	-	18.18	5.80	31.87

Globally, the parity plot (Fig. S7.11) shows that the developed model fits well the experimental concentration of EL.

The residual analysis (Figs S7.12-S7.15) shows that the residuals are normally distributed versus the events, time, simulated and experimental EL concentrations. These normal distributions confirm that the developed model is correct.

Fig. 5 shows the fit of the model to some experimental concentrations of EL with the 95% prediction intervals and the mean estimated values. From Fig. 5, one can notice that the model fits well the experimental concentrations, and most of the experimental concentrations lie between the intervals. The developed model can correctly simulate the kinetics and the equilibrium phase.

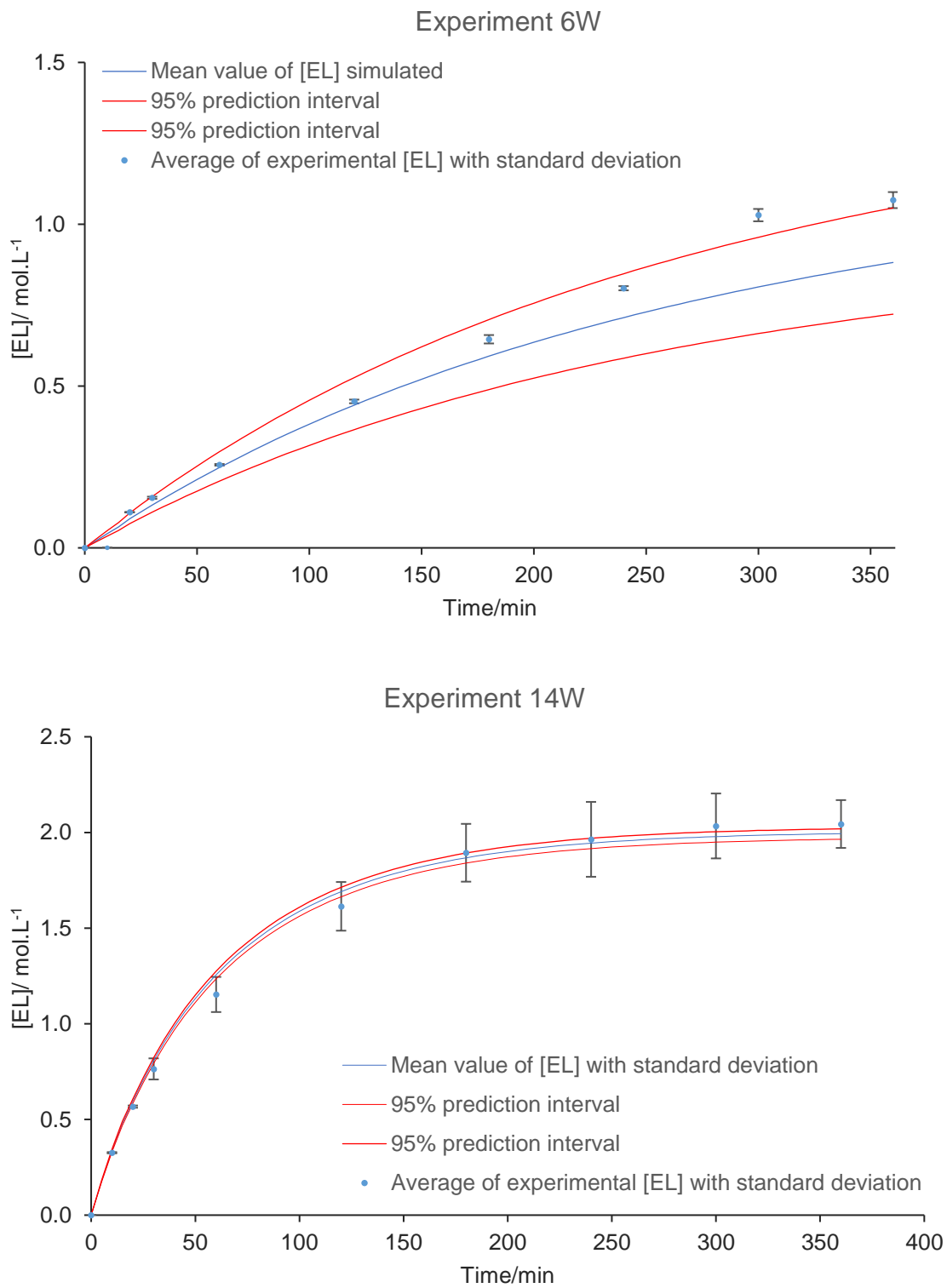


Fig. 5. Fit of Model to the experimental concentrations with prediction intervals for the synthesis of EL in water solvent.

3.4 Explanation of solvent effect on kinetics

Using the kinetics and equilibrium constants obtained previously (Tables 6-8), we simulated reactant and product concentrations and the reaction rate of three experiments carried out in similar operating conditions in each solvent (Table S8.1). In these experiments, sulfuric acid and LA concentrations were similar.

Figs. 6 A&B show that the esterification rate is faster in ethanol solvent. At 50°C, the initial reaction rate in ethanol is ca. 8 times faster than in water solvent. The same thing can be observed at 70°C, where the esterification rate of water is still the lowest: 4 times slower than in GVL and 6 times in ethanol solvent.

Both at 50°C and 70°C (Fig. 6.A&B), one can observe that the initial kinetics in ethanol is faster than in GVL solvents, even if the difference is not that remarkable since at 50°C, the esterification rate is 1.5 times higher than in ethanol.

Figs. 6 C&D show that maximum EL yields are obtained in ethanol solvent. At 70°C, the final concentration of EL represents 99% of the initial concentration of LA in ethanol compared to 71% for the water solvent.

However, the benefits of using GVL solvent are its highest boiling point, allowing experiments at higher temperatures to increase the reaction rate.

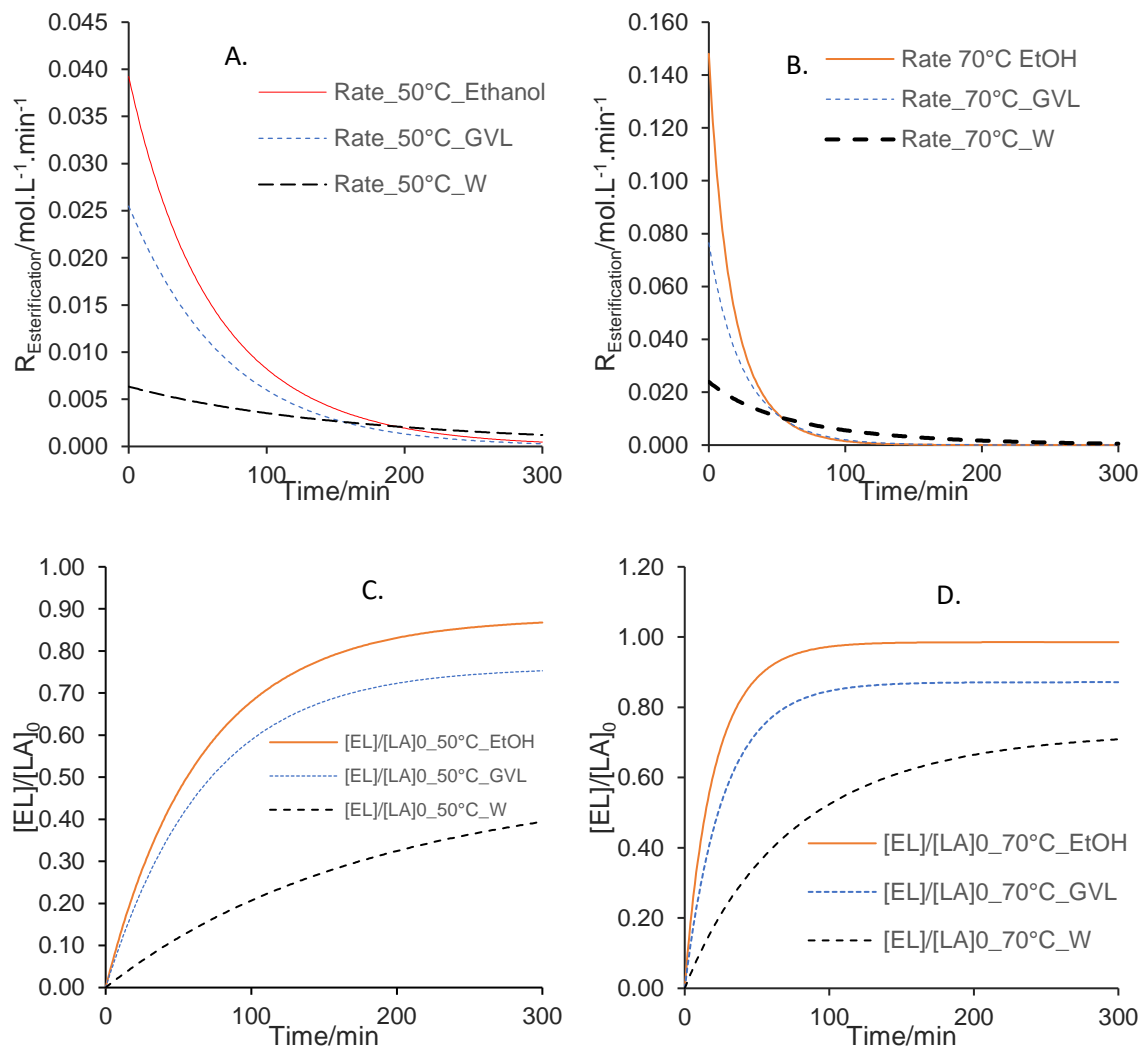


Fig. 6. Temperature and solvent effect on esterification reaction rate and ratio $\frac{[\text{EL}]}{[\text{LA}]_0}$.

The Kamlet-Abboud-Taft equation was used to find the relationships between solvent properties and kinetics. The solvatochromic solvent parameters (Table 4) were used in Eq.(8). The parameters (s, a and b) of Eq.(8) were estimated by using the solver DDAPLUS, implemented in Athena Visual Studio. The responses were the natural logarithm of the estimated constants at different temperatures from Tables 6-8. Fig. 7 shows the parity plot between the estimated values of $\ln(k_C^{\text{Solvent}})_{\text{Sim}}$ and the ones obtained from the regression using Kamlet-Abboud-Taft equation $\ln(k_C^{\text{Solvent}})_{\text{KAT}}$. One

can notice that KAT equation can predict the kinetic constant in different solvents. Table 9 shows the values of A_0 , s , a and b at different temperatures (Eq. (8)). From Table 9, one can notice that solvent effect on the rate constant is mainly due to its ability to accept hydrogen-bond (measured by b value) and its ability to stabilize a charge (measured by s value). These two properties have antagonist effect on the rate constant value. The solvent ability to donate hydrogen-bond has less influenced (measured by a) on the rate constant value.

The negative values of s means that solvents with a high ability to stabilize a charge decrease the kinetic constants, whereas the positive value of b means that hydrogen-bond acceptor solvents increase the kinetic constants. Thus, solvents with low values for π^* and high values for β should be favored for the acid-catalyzed esterification. Solvents that can stabilize a charge could stabilize the carbocation intermediate Int1 and/or proton (Figs S4.1 and S4.2), decreasing their reactivities.

Table 9. Values of A_0 , s , a and b of KAT equation (Eq. (8)).

Temperature/°C	A_0	s	a	b
50	-0.252	-7.413	2.062	6.536
52	-0.319	-7.343	2.082	6.736
54	-0.387	-7.274	2.101	6.936
56	-0.032	-7.411	2.138	6.737
58	-0.050	-7.366	2.159	6.887
60	-0.069	-7.322	2.179	7.036
62	-0.087	-7.278	2.200	7.183
64	-0.105	-7.235	2.219	7.327
66	-0.123	-7.192	2.239	7.471
68	-0.140	-7.150	2.258	7.612
70	-0.158	-7.108	2.278	7.752

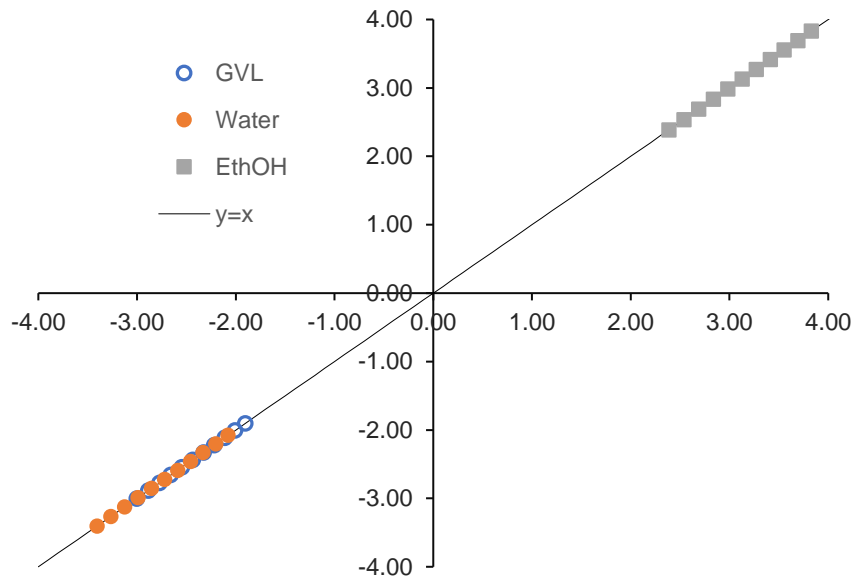


Fig. 7. Parity plot $\ln(k_C^{\text{Solvent}})_{\text{Calculated from Model}}$ versus $A_0 + s \cdot \pi^* + a \cdot \alpha + b \cdot \beta$ for each solvent and different temperatures (Table 9).

4 Conclusions

This manuscript proposes a kinetic investigation to synthesize ethyl levulinate via the acid-catalyzed esterification of levulinic by sulfuric acid in three solvents: ethanol solvent (polar protic), GVL solvent (polar aprotic) and water solvent (polar protic). In order to perform a fair comparison, kinetic models were developed for each solvent at different temperatures, reactant, product and catalyst concentrations, and by taking into account the proton concentration. ePC-SAFT approach was used to estimate the sulfuric acid first dissociation in GVL solvent and ethanol solvent. Bayesian inference was used to evaluate the credible intervals of the estimated constants for each model. The developed models were found to be reliable.

In the absence of sulfuric acid, the reaction rate was found to be negligible in solvents. The esterification rate follows the order: $r_{esterification}^{Ethanol} > r_{esterification}^{GVL} > r_{esterification}^{Water}$. The conversion at the equilibrium follows the same order. For instance, at 70°C, the initial rate in ethanol solvent, GVL solvent and water solvent was calculated to be 0.15, 0.08 and 0.02 mol.L⁻¹.min⁻¹, respectively; the conversion of LA at equilibrium in ethanol and GVL solvents was calculated to be respectively 99% and 87% compared to 71% in water solvent at 70°C.

Based on the developed kinetic models, the Kamlet-Abboud-Taft linear solvation energy was used to establish a relationship between kinetics and solvent properties in different solvents and reaction temperatures. Solvents able to stabilize a charge could stabilize the cation transition state and proton, decreasing the reactivity of these species and thus decreasing the kinetics.

This work proposed a first methodology for solvent selection for the esterification of LA by ethanol by evaluating the contribution of polarizability, H donor and acceptor capacity. By knowing the KAT properties of a solvent, one can predict the kinetics in this solvent. One can also use this information to choose the most appropriate solvent to get faster kinetics. Solvent with low polarizability capacity and high hydrogen-bond donor capacity should be used for LA esterification over acid catalyst. The continuation of this work could be the kinetic study over heterogeneous and the temperature dependence of solvatochromic parameters.

Notation

A_0	Regression value for Kamlet-Abboud-Taft equation
a	Regression parameter for Kamlet-Abboud-Taft equation
b	Regression parameter for Kamlet-Abboud-Taft equation
C_{LA}	Concentration of LA
$C_{Ethanol}$	Concentration of ethanol
C_{EL}	Concentration of ethyl levulinate
C_W	Concentration of water
c_p^0	Specific standard heat capacity used in Eq.17
E_a^{GVL}	Activation energy of LA esterification in GVL solvent
$E_a^{Ethanol}$	Activation energy for LA esterification in excess of ethanol
E_a^W	Activation energy for LA esterification in excess of water
$f_u(\theta)$	Simulated value for EL
ΔH_r^0	Standard reaction enthalpy
ΔH_{II}^0	Standard reaction enthalpy used in Eq.17
ΔH_r^{GVL}	Reaction enthalpy for LA esterification in GVL solvent
$\Delta H_r^{Ethanol}$	Reaction enthalpy for LA esterification in excess of ethanol
ΔH_r^W	Reaction enthalpy for LA esterification in excess of water
K_I	First dissociation constant for H ₂ SO ₄
K_{II}	Second dissociation constant for H ₂ SO ₄
K_{III}	Dissociation constant for LA
K_{II}^T	Second dissociation constant for H ₂ SO ₄

K_{II}^O	Second standard dissociation constant for H ₂ SO ₄
K_C^{GVL}	Equilibrium constant based on concentration of LA esterification in GVL solvent
$K_C^{Ethanol}$	Equilibrium constant based on concentration of LA esterification in excess of ethanol
K_C^W	Equilibrium constant based on concentration on LA esterification in excess of water
K_x	Mole-fraction ratio at equilibrium or ‘apparent’ equilibrium constant
k_C^{GVL}	Rate constant based on concentration for LA esterification in GVL solvent
$k_C^{Ethanol}$	Rate constant based on concentration for LA esterification in excess of ethanol
k_C^W	Rate constant based on concentration for LA esterification in excess of water
$k_C^{Solvent}$	Rate constant in a solvent
k_{ij}	Binary interaction parameters used in modeling ePC-SAFT
p	pressure
pK _a	dissociation constant
pK_a^x	Dissociation constant based on molar fraction
pK_a^C	Dissociation constant based on concentration used in Eq.5
pK_a^a	Dissociation constant based on activity used in Eq.4
R	Universal gas constant
$r_{esterification}^{GVL}$	LA esterification rate in GVL solvent
$r_{esterification}^{Ethanol}$	LA esterification rate in excess of ethanol
$r_{esterification}^W$	LA esterification rate in excess of water
$S(\theta)$	Objective function minimized with Athena Visual Studio
s	Regression parameter for Kamlet-Abboud-Taft equation
T	Temperature

T_0	Reference standard temperature used in Eq.17
$T_{th,1}$	Equilibrium constant of first H ₂ SO ₄ dissociation
$T_{th,2}$	Equilibrium constant of second H ₂ SO ₄ dissociation
x	Molar fraction
y_u	Experimental value for EL

Greek letters

α	Solvatochromic solvent parameter in Kamlet-Abboud-Taft equation for the solvent hydrogen-bond donor acidity
β	Solvatochromic solvent parameter in Kamlet-Abboud-Taft equation for solvent hydrogen-bond acceptor basicity
γ_i	Activity coefficient
γ_i^*	Rational activity coefficient
ϵ_r	Relative permittivity
$\epsilon_{r,DMF}$	Relative permittivity of H ₂ SO ₄ in DMF
$\epsilon_{r,DMSO}$	Relative permittivity of H ₂ SO ₄ in DMSO
θ	Estimated parameter
π^*	Solvatochromic solvent parameter in Kamlet-Abboud-Taft equation for polarizability

Abbreviations

ACN	Acetonitrile
DMF	Dimethylformamide
DMSO	Dimethyl sulfoxide

EL	Ethyl levulinate
EtOH	Ethanol
GVL	γ -valerolactone
HBA	Hydrogen bond acceptor
HBD	Hydrogen bond donor
HPD	Highest probability density in modeling estimation estimation
KAT	Kamlet-Abboud-Taft
LA	Levulinic acid
LCB	Lignocellulosic biomass
ODE	Ordinary differential equation
W	Water

Declaration of Competing Interest

The authors report no declarations of interest.

Acknowledgments

The authors thank INSA Rouen Normandy, University of Rouen Normandy, the Centre National de la Recherche Scientifique (CNRS), European Regional Development Fund (ERDF) N° HN0001343, Labex SynOrg (ANR-11-LABX-0029), Carnot Institute I2C, the graduate school for reasearch XL-Chem (ANR-18-EURE-0020 XL CHEM) and Region Normandie for their support. GC/FID was financed by ERDF RIN Green Chem 2019NU01FOBC08 N° 17P04374.

The authors thank the Maîtrise des Risques et Environementaux department, and the Erasmus programme to make the research projects of Sindi Baco and Rashid Ismail Bedawi Zakaria possible. This research was funded, in whole or in part, by the ANR (French National Research Agency) and the DFG (German Research Foundation) through the project MUST (MicroflUidics for Structure-reactivity relationships aided by Thermodynamics & kinetics) [ANR-20-CE92-0002-01 - Project number 446436621].

References

- Aaron, J.J., Maafi, M., Kersebet, C., Párkányi, C., Antonious, M.S., Motohashi, N., 1996. A solvatochromic study of new benzo[a]phenothiazines for the determination of dipole moments and specific solute-solvent interactions in the first excited singlet state. *J. Photochem. Photobiol. A Chem.* 101, 127–136.
[https://doi.org/10.1016/S1010-6030\(96\)04442-5](https://doi.org/10.1016/S1010-6030(96)04442-5)
- Aaron, J.J., Maafi, M., Párkányi, C., Boniface, C., 1995. Quantitative treatment of the solvent effects on the electronic absorption and fluorescence spectra of acridines and phenazines. The ground and first excited singlet-state dipole moments. *Spectrochim. Acta Part A Mol. Spectrosc.* 51, 603–615. [https://doi.org/10.1016/0584-8539\(94\)00164-7](https://doi.org/10.1016/0584-8539(94)00164-7)
- Alonso, D.M., Wettstein, S.G., Dumesic, J.A., 2013. Gamma-valerolactone, a sustainable platform molecule derived from lignocellulosic biomass. *Green Chem.* 15, 584–595.
<https://doi.org/10.1039/C3GC37065H>
- Auxenfans, T., Husson, E., Sarazin, C., 2017. Simultaneous pretreatment and enzymatic saccharification of (ligno) celluloses in aqueous-ionic liquid media: A compromise. *Biochem. Eng. J.* 117, 77–86. <https://doi.org/10.1016/j.bej.2016.10.004>
- Badgujar, K.C., Badgujar, V.C., Bhanage, B.M., 2020. A review on catalytic synthesis of energy rich fuel additive levulinate compounds from biomass derived levulinic acid. *Fuel Process. Technol.* 197, 106213.
<https://doi.org/10.1016/J.FUPROC.2019.106213>
- Bhat, N.S., Mal, S.S., Dutta, S., 2021. Recent advances in the preparation of levulinic esters from biomass-derived furanic and levulinic chemical platforms using

heteropoly acid (HPA) catalysts. *Mol. Catal.* 505, 111484.

<https://doi.org/10.1016/J.MCAT.2021.111484>

Bülow, M., Ascani, M., Held, C., 2021. ePC-SAFT advanced - Part I: Physical meaning of including a concentration-dependent dielectric constant in the born term and in the Debye-Hückel theory. *Fluid Phase Equilib.* 535, 112967.

<https://doi.org/10.1016/j.fluid.2021.112967>

Buzzi-Ferraris, G., 1999. Planning of experiments and kinetic analysis. *Catal. Today* 52, 125–132. [https://doi.org/10.1016/S0920-5861\(99\)00070-X](https://doi.org/10.1016/S0920-5861(99)00070-X)

Cameretti, L.F., Sadowski, G., Mollerup, J.M., 2005. Modeling of aqueous electrolyte solutions with perturbed-chain statistical associated fluid theory. *Ind. Eng. Chem. Res.* 44, 3355–3362. <https://doi.org/10.1021/ie0488142>

Capecci, S., Wang, Y., Casson Moreno, V., Held, C., Leveneur, S., 2021a. Solvent effect on the kinetics of the hydrogenation of n-butyl levulinate to γ -valerolactone. *Chem. Eng. Sci.* 231, 116315. <https://doi.org/10.1016/j.ces.2020.116315>

Capecci, S., Wang, Y., Delgado, J., Moreno, V.C., Mignot, M., Grénman, H., Murzin, D.Y., Leveneur, S., 2021b. Bayesian Statistics to Elucidate the Kinetics of γ -Valerolactone from n-Butyl Levulinate Hydrogenation over Ru/C. *Ind. Eng. Chem. Res.* 60, 11725–11736. <https://doi.org/10.1021/ACS.IECR.1C02107>

Caracotsios, M., Stewart, W.E., 1985. Sensitivity analysis of initial value problems with mixed odes and algebraic equations. *Comput. Chem. Eng.* 9, 359–365.

[https://doi.org/10.1016/0098-1354\(85\)85014-6](https://doi.org/10.1016/0098-1354(85)85014-6)

Da Silva, M.J., Chaves, D.M., Teixeira, M.G., Oliveira Bruziquesi, C.G., 2021.

Esterification of levulinic acid over Sn(II) exchanged Keggin heteropolyacid salts:

An efficient route to obtain bioaditives. *Mol. Catal.* 504, 111495.

<https://doi.org/10.1016/J.MCAT.2021.111495>

- Delgado, J., Vasquez Salcedo, W.N., Bronzetti, G., Casson Moreno, V., Mignot, M., Legros, J., Held, C., Grénman, H., Leveneur, S., 2022. Kinetic model assessment for the synthesis of γ -valerolactone from n-butyl levulinate and levulinic acid hydrogenation over the synergy effect of dual catalysts Ru/C and Amberlite IR-120. *Chem. Eng. J.* 430, 133053. <https://doi.org/10.1016/j.cej.2021.133053>
- Di Menno Di Bucchianico, D., Wang, Y., Buvat, J.C., Pan, Y., Casson Moreno, V., Leveneur, S., 2022. Production of levulinic acid and alkyl levulinates: A process insight. *Green Chem.* <https://doi.org/10.1039/d1gc02457d>
- Di, X., Zhang, Y., Fu, J., Yu, Q., Wang, Z., Yuan, Z., 2019. Biocatalytic upgrading of levulinic acid to methyl levulinate in green solvents. *Process Biochem.* 81, 33–38. <https://doi.org/10.1016/j.procbio.2019.03.024>
- Garcia-Hernandez, E.A., Souza, C.R., Vernières-Hassimi, L., Leveneur, S., 2019. Kinetic modeling using temperature as an on-line measurement: Application to the hydrolysis of acetic anhydride, a revisited kinetic model. *Thermochim. Acta* 682. <https://doi.org/10.1016/j.tca.2019.178409>
- García-Río, L., Leis, J.R., Iglesias, E., 1997. Nitrosation of Amines in Nonaqueous Solvents. 2. Solvent-Induced Mechanistic Changes. *J. Org. Chem.* 62, 4712–4720. <https://doi.org/10.1021/jo9701896>
- Gross, J., Sadowski, G., 2001. Perturbed-chain SAFT: An equation of state based on a perturbation theory for chain molecules. *Ind. Eng. Chem. Res.* 40, 1244–1260. <https://doi.org/10.1021/ie0003887>

- Holzweber, M., Lungwitz, R., Doerfler, D., Spange, S., Koel, M., Hutter, H., Linert, W., 2013. Mutual lewis acid-base interactions of cations and anions in ionic liquids. *Chem. - A Eur. J.* 19, 288–293. <https://doi.org/10.1002/chem.201201978>
- Islam, T., Islam Sarker, M.Z., Uddin, A.H., Yunus, K. Bin, Prasad, R., Mia, M.A.R., Ferdosh, S., 2020. Kamlet Taft Parameters: A Tool to Alternate the Usage of Hazardous Solvent in Pharmaceutical and Chemical Manufacturing/Synthesis - A Gateway towards Green Technology. *Anal. Chem. Lett.* 10, 550–561. <https://doi.org/10.1080/22297928.2020.1860124>
- Izutsu, K., 2009. *Electrochemistry in Nonaqueous Solutions: Second Edition.* *Electrochem. Nonaqueous Solut.* Second Ed. 1–415. <https://doi.org/10.1002/9783527629152>
- Izutsu, K., 2003. Acid-Base Reactions in Non-Aqueous Solvents. *Electrochem. Nonaqueous Solut.* 59–83. <https://doi.org/10.1002/3527600655.CH3>
- Jabbari, M., Gharib, F., 2012. Solvent dependence on antioxidant activity of some water-insoluble flavonoids and their cerium(IV) complexes. *J. Mol. Liq.* 168, 36–41. <https://doi.org/10.1016/j.molliq.2012.02.001>
- Janssen, A.E.M., Sjursnes, B.J., Vakurov, A. V., Halling, P.J., 1999. Kinetics of lipase-catalyzed esterification in organic media: Correct model and solvent effects on parameters. *Enzyme Microb. Technol.* 24, 463–470. [https://doi.org/10.1016/S0141-0229\(98\)00134-3](https://doi.org/10.1016/S0141-0229(98)00134-3)
- Jessop, P.G., Jessop, D.A., Fu, D., Phan, L., 2012. Solvatochromic parameters for solvents of interest in green chemistry. *Green Chem.* 14, 1245–1259. <https://doi.org/10.1039/C2GC16670D>

- Joshi, H., Moser, B.R., Toler, J., Smith, W.F., Walker, T., 2011. Ethyl levulinate: A potential bio-based diluent for biodiesel which improves cold flow properties. *Biomass and Bioenergy* 35, 3262–3266.
<https://doi.org/10.1016/J.BIOMBIOE.2011.04.020>
- Kamlet, M.J., Abboud, J.L.M., Taft, R.W., 1981. An Examination of Linear Solvation Energy Relationships, in: *Progress in Physical Organic Chemistry*. John Wiley & Sons, Ltd, pp. 485–630. <https://doi.org/10.1002/9780470171929.ch6>
- Knopf, D.A., Luo, B.P., Krieger, U.K., Koop, T., 2003. Thermodynamic dissociation constant of the bisulfate ion from Raman and ion interaction modeling studies of aqueous sulfuric acid at low temperatures. *J. Phys. Chem. A* 107, 4322–4332.
<https://doi.org/10.1021/jp027775+>
- Kolthof, I.M., Chantooni, M.K., 1999. Dissociation constant, K_a , and stability constant, $K(\text{HA}_2^-)$, of the 1:1 Homoconjugate of sulfuric and nitric acids in acetonitrile at 298.1 K. revised values. *J. Chem. Eng. Data* 44, 124–129.
<https://doi.org/10.1021/je9801922>
- Kolthoff, I.M. (Izaak M., Elving, P.J., 1959. *Treatise on analytical chemistry*.
- Kopetzki, D., Antonietti, M., 2010. Transfer hydrogenation of levulinic acid under hydrothermal conditions catalyzed by sulfate as a temperature-switchable base. *Green Chem.* 12, 656–660. <https://doi.org/10.1039/B924648G>
- Laurence, C., Legros, J., Chantzis, A., Planchat, A., Jacquemin, D., 2015. A Database of dispersion-induction DI, electrostatic ES, and hydrogen bonding α_1 and δ_1 solvent parameters and some applications to the multiparameter correlation analysis of solvent effects. *J. Phys. Chem. B* 119, 3174–3184.

https://doi.org/10.1021/JP512372C/SUPPL_FILE/JP512372C_SI_001.PDF

- Lemberg, M., Sadowski, G., 2017. Predicting the Solvent Effect on Esterification Kinetics. *ChemPhysChem* 18, 1977–1980. <https://doi.org/10.1002/cphc.201700507>
- Leveneur, S., Salmi, T., Murzin, D.Y., Estel, L., Wärnå, J., Musakka, N., 2008. Kinetic study and modeling of peroxypropionic acid synthesis from propionic acid and hydrogen peroxide using homogeneous catalysts. *Ind. Eng. Chem. Res.* 47, 656–664. <https://doi.org/10.1021/ie070670e>
- Li, Z., Zuo, M., Jiang, Y., Tang, X., Zeng, X., Sun, Y., Lei, T., Lin, L., 2016. Stable and efficient CuCr catalyst for the solvent-free hydrogenation of biomass derived ethyl levulinate to γ -valerolactone as potential biofuel candidate. *Fuel* 175, 232–239. <https://doi.org/10.1016/J.FUEL.2016.02.051>
- Liu, Y., Lotero, E., Goodwin, J.G., 2006. Effect of water on sulfuric acid catalyzed esterification. *J. Mol. Catal. A Chem.* 245, 132–140. <https://doi.org/10.1016/j.molcata.2005.09.049>
- Lotti, M., Pleiss, J., Valero, F., Ferrer, P., 2015. Effects of methanol on lipases: Molecular, kinetic and process issues in the production of biodiesel. *Biotechnol. J.* 10, 22–30. <https://doi.org/10.1002/biot.201400158>
- Lu, J., Brown, J.S., Boughner, E.C., Liotta, C.L., Eckert, C.A., 2002a. Solvatochromic Characterization of Near-Critical Water as a Benign Reaction Medium. *Ind. Eng. Chem. Res.* 41, 2835–2841. <https://doi.org/10.1021/IE020160E>
- Lu, J., Brown, J.S., Boughner, E.C., Liotta, C.L., Eckert, C.A., 2002b. Solvatochromic characterization of near-critical water as a benign reaction medium. *Ind. Eng. Chem. Res.* 41, 2835–2841. <https://doi.org/10.1021/ie020160e>

- Marcus, Y., 2006. Are solubility parameters relevant to supercritical fluids? *J. Supercrit. Fluids* 38, 7–12. <https://doi.org/10.1016/j.supflu.2005.11.008>
- Melchiorre, M., Amendola, R., Benessere, V., Cucciolito, M.E., Ruffo, F., Esposito, R., 2020. Solvent-free transesterification of methyl levulinate and esterification of levulinic acid catalyzed by a homogeneous iron(III) dimer complex. *Mol. Catal.* 483, 110777. <https://doi.org/10.1016/J.MCAT.2020.110777>
- Mellmer, M.A., Sener, C., Gallo, J.M.R., Luterbacher, J.S., Alonso, D.M., Dumesic, J.A., 2014. Solvent Effects in Acid-Catalyzed Biomass Conversion Reactions. *Angew. Chemie Int. Ed.* 53, 11872–11875. <https://doi.org/10.1002/ANIE.201408359>
- Nikolć, J.B., Ušćumlić, G.S., Juranić, I.O., 2010. A linear solvation energy relationship study for the reactivity of 2-(4-substituted phenyl)-cyclohe-1-enecarboxylic, 2-(4-substituted phenyl)-benzoic, and 2-(4-substituted phenyl)-acrylic acids with diazodiphenylmethane in various solvents. *Int. J. Chem. Kinet.* 42, 430–439. <https://doi.org/10.1002/KIN.20497>
- Párkányi, C., Boniface, C., Aaron, J.J., Maafi, M., 1993. A quantitative study of the effect of solvent on the electronic absorption and fluorescence spectra of substituted phenothiazines: evaluation of their ground and excited singlet-state dipole moments. *Spectrochim. Acta Part A Mol. Spectrosc.* 49, 1715–1725. [https://doi.org/10.1016/0584-8539\(93\)80239-7](https://doi.org/10.1016/0584-8539(93)80239-7)
- Paul, S., Heng, P.W.S., Chan, L.W., 2013. Optimization in solvent selection for chlorin e6 in photodynamic therapy. *J. Fluoresc.* 23, 283–291. <https://doi.org/10.1007/s10895-012-1146-x>
- Peixoto, A.F., Ramos, R., Moreira, M.M., Soares, O.S.G.P., Ribeiro, L.S., Pereira,

- M.F.R., Delerue-Matos, C., Freire, C., 2021. Production of ethyl levulinate fuel bioadditive from 5-hydroxymethylfurfural over sulfonic acid functionalized biochar catalysts. *Fuel* 303, 121227. <https://doi.org/10.1016/J.FUEL.2021.121227>
- Peng, L., Gao, X., Chen, K., 2015. Catalytic upgrading of renewable furfuryl alcohol to alkyl levulinates using AlCl_3 as a facile, efficient, and reusable catalyst. *Fuel* 160, 123–131. <https://doi.org/10.1016/J.FUEL.2015.07.086>
- Piskun, A.S., van de Bovenkamp, H.H., Rasrendra, C.B., Winkelman, J.G.M., Heeres, H.J., 2016. Kinetic modeling of levulinic acid hydrogenation to γ -valerolactone in water using a carbon supported Ru catalyst. *Appl. Catal. A Gen.* 525, 158–167. <https://doi.org/10.1016/j.apcata.2016.06.033>
- Pyrgakis, K.A., Kokossis, A.C., 2018. An Engineering Tool to Screen and Integrate Biomass Valorization Paths in Multiple-Feedstock Biorefineries, in: *Computer Aided Chemical Engineering*. Elsevier, pp. 573–578. <https://doi.org/10.1016/B978-0-444-64235-6.50103-0>
- Raducan, A., Cantemir, A.R., Puiu, M., Oancea, D., 2012. Kinetics of hydrogen peroxide decomposition by catalase: Hydroxylic solvent effects. *Bioprocess Biosyst. Eng.* 35, 1523–1530. <https://doi.org/10.1007/s00449-012-0742-0>
- Rauf, M.A., Hisaindee, S., Graham, J.P., Nawaz, M., 2012. Solvent effects on the absorption and fluorescence spectra of Cu(II)-phthalocyanine and DFT calculations. *J. Mol. Liq.* 168, 102–109. <https://doi.org/10.1016/j.molliq.2012.01.008>
- Riechert, O., Husham, M., Sadowski, G., Zeiner, T., 2015. Solvent effects on esterification equilibria. *AIChE J.* 61, 3000–3011. <https://doi.org/10.1002/aic.14873>
- Russo, V., Tesser, R., Rossano, C., Cogliano, T., Vitiello, R., Leveneur, S., Di Serio, M.,

2020. Kinetic study of Amberlite IR120 catalyzed acid esterification of levulinic acid with ethanol: From batch to continuous operation. *Chem. Eng. J.* 401, 126126. <https://doi.org/10.1016/J.CEJ.2020.126126>
- Shen, X.R., Xia, D.Z., Xiang, Y.X., Gao, J.G., 2019. γ -valerolactone (GVL) as a bio-based green solvent and ligand for iron-mediated AGET ATRP. *E-Polymers* 19, 323–329. https://doi.org/10.1515/EPOLY-2019-0033/DOWNLOADASSET/SUPPL/EPOLY-2019-0033_SM.PDF
- Sherwood, J., Granelli, J., McElroy, C.R., Clark, J.H., 2019. A Method of Calculating the Kamlet–Abboud–Taft Solvatochromic Parameters Using COSMO-RS. *Mol.* 2019, Vol. 24, Page 2209 24, 2209. <https://doi.org/10.3390/MOLECULES24122209>
- Shinde, S.H., Hengne, A., Rode, C. V., 2019. Lignocellulose-derived platform molecules: An introduction, in: *Biomass, Biofuels, Biochemicals: Recent Advances in Development of Platform Chemicals*. Elsevier, pp. 1–31. <https://doi.org/10.1016/B978-0-444-64307-0.00001-9>
- Singhvi, M.S., Gokhale, D. V., 2019. Lignocellulosic biomass: Hurdles and challenges in its valorization. *Appl. Microbiol. Biotechnol.* <https://doi.org/10.1007/s00253-019-10212-7>
- Sippola, H., 2013. Critical evaluation of the second dissociation constants for aqueous sulfuric acid over a wide temperature range. *J. Chem. Eng. Data* 58, 3009–3032. https://doi.org/10.1021/JE4004614/ASSET/IMAGES/LARGE/JE-2013-004614_0019.JPEG
- Sippola, H., Taskinen, P., 2014. Thermodynamic properties of aqueous sulfuric acid. *J. Chem. Eng. Data* 59, 2389–2407. <https://doi.org/10.1021/je4011147>

- Stewart, W.E., Caracotsios, M., 2008. Computer-Aided Modeling of Reactive Systems, First. ed, Computer-Aided Modeling of Reactive Systems. New Jersey.
<https://doi.org/10.1002/9780470282038>
- Thadathil, D.A., Varghese, S., Akshaya, K.B., Thomas, R., Varghese, A., 2019. An Insight into Photophysical Investigation of (E)-2-Fluoro-N³-(1-(4-Nitrophenyl)Ethylidene)Benzohydrazide through Solvatochromism Approaches and Computational Studies. *J. Fluoresc.* 29, 1013–1027. <https://doi.org/10.1007/s10895-019-02415-y>
- Tian, M., McCormick, R.L., Luecke, J., de Jong, E., van der Waal, J.C., van Klink, G.P.M., Boot, M.D., 2017. Anti-knock quality of sugar derived levulinic esters and cyclic ethers. *Fuel* 202, 414–425. <https://doi.org/10.1016/J.FUEL.2017.04.027>
- Toch, K., Thybaut, J.W., Marin, G.B., 2015. A systematic methodology for kinetic modeling of chemical reactions applied to n-hexane hydroisomerization. *AIChE J.* 61, 880–892. <https://doi.org/10.1002/aic.14680>
- Ušcumlić, G.S., Nikolić, J.B., 2009. The study of linear solvation energy relationship for the reactivity of carboxylic acids with diazodiphenylmethane in protic and aprotic solvents. *J. Serbian Chem. Soc.* <https://doi.org/10.2298/JSC0912335U>
- van Zandvoort, I., Wang, Y., Rasrendra, C.B., van Eck, E.R.H., Bruijninx, P.C.A., Heeres, H.J., Weckhuysen, B.M., 2013. Formation, Molecular Structure, and Morphology of Humins in Biomass Conversion: Influence of Feedstock and Processing Conditions. *ChemSusChem* 6, 1745–1758.
<https://doi.org/10.1002/CSSC.201300332>
- Voges, M., Schmidt, F., Wolff, D., Sadowski, G., Held, C., 2016. Thermodynamics of the

alanine aminotransferase reaction. *Fluid Phase Equilib.* 422, 87–98.

<https://doi.org/10.1016/j.fluid.2016.01.023>

Wang, Y., Cipolletta, M., Vernières-Hassimi, L., Casson-Moreno, V., Leveneur, S., 2019.

Application of the concept of Linear Free Energy Relationships to the hydrogenation of levulinic acid and its corresponding esters. *Chem. Eng. J.* 374, 822–831.

<https://doi.org/10.1016/j.cej.2019.05.218>

Weiß, N., Schmidt, C.H., Thielemann, G., Heid, E., Schröder, C., Spange, S., 2021. The

physical significance of the Kamlet-Taft: π^* parameter of ionic liquids. *Phys.*

Chem. Chem. Phys. 23, 1616–1626. <https://doi.org/10.1039/d0cp04989a>

Williams, R., 2022. pKa Data compiled by R. Williams [WWW Document]. Res.

psu.edu/brpgroup/pKa_compilation.pdf. URL

https://organicchemistrydata.org/hansreich/resources/pka/pka_data/pka-compilation-williams.pdf (accessed 5.27.22).

Windom, B.C., Lovestead, T.M., Mascal, M., Nikitin, E.B., Bruno, T.J., 2011. Advanced

Distillation Curve Analysis on Ethyl Levulinate as a Diesel Fuel Oxygenate and a Hybrid Biodiesel Fuel. *Energy and Fuels* 25, 1878–1890.

<https://doi.org/10.1021/EF200239X>

Wu, Y., Lawson, P.D. V., Henary, M.M., Schmidt, K., Brédas, J.L., Fahrni, C.J., 2007.

Excited state intramolecular proton transfer in 2-(2'-

arylsulfonamidophenyl)benzimidazole derivatives: insights into the origin of donor substituent-induced emission energy shifts. *J. Phys. Chem. A* 111, 4584–4595.

<https://doi.org/10.1021/jp068832s>

Yan, K., Yang, Y., Chai, J., Lu, Y., 2015. Catalytic reactions of gamma-valerolactone: A

platform to fuels and value-added chemicals. *Appl. Catal. B Environ.* 179, 292–304.

<https://doi.org/10.1016/j.apcatb.2015.04.030>

Zainol, M.M., Amin, N.A.S., Asmadi, M., 2019. Kinetics and thermodynamic analysis of levulinic acid esterification using lignin-furfural carbon cryogel catalyst. *Renew. Energy* 130, 547–557. <https://doi.org/10.1016/J.RENENE.2018.06.085>

<https://doi.org/10.1016/J.RENENE.2018.06.085>

Zhao, L., Sun, Z.F., Zhang, C.C., Nan, J., Ren, N.Q., Lee, D.J., Chen, C., 2022. Advances in pretreatment of lignocellulosic biomass for bioenergy production: Challenges and perspectives. *Bioresour. Technol.* 343, 126123.

<https://doi.org/10.1016/J.BIORTECH.2021.126123>